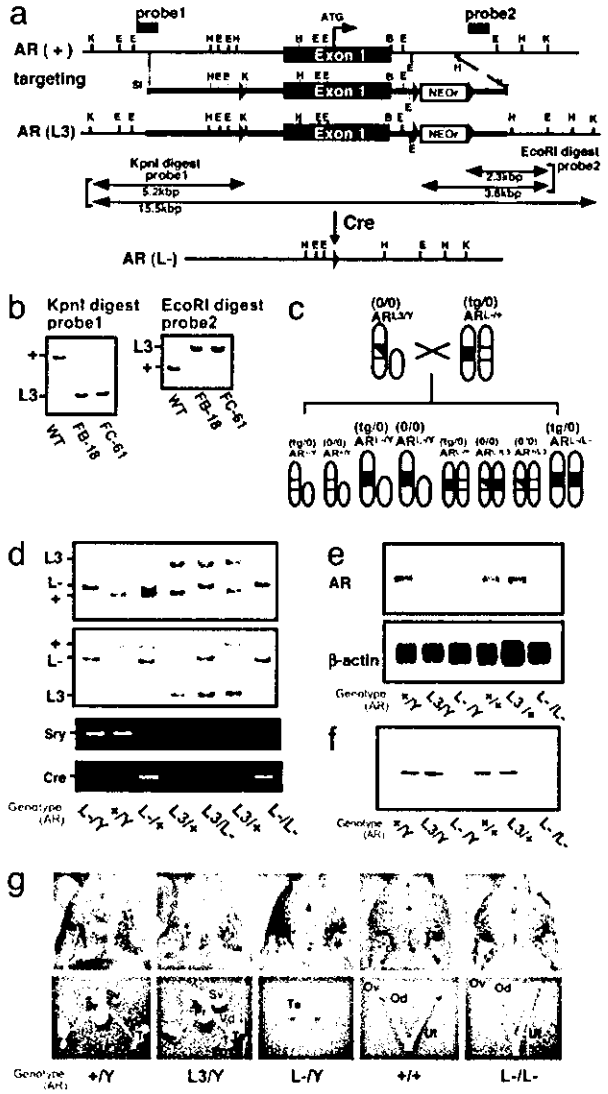

Fig. 1. Establishment of the AR-null mutant mouse line. (*a*) Diagram of the wild-type AR genomic locus (+), the floxed *AR* L3 allele (L3), and the *AR* allele (L−) obtained after Cre-mediated excision of exon 1. K, *KpnI*; E, *EcoRI*; H, *HindIII*; B, *BamHI*; LoxP sites are indicated as black arrowheads. The targeting vector consisted of a 7.6-kb 5′ homologous region containing exon 1, a 1.3-kb 3′ homologous region, a single loxP site, and the neo cassette with two loxP sites. (*b*) Southern blot analysis of targeted embryonic stem clones. Genomic DNA from WT TT2 embryonic stem cells (WT) and homologous targeted clones (FB-18 and FC-61) were digested with *KpnI* for hybridization with probe 1 or with *EcoRI* for hybridization with probe 2. (*c*) Strategy for the disruption of the floxed *AR* gene by using the CMV-Cre transgene. $AR^{L3/Y}$ mice were crossed with CMV-$Cre^{(tg/0)}/AR^{L-/+}$ mice to generate CMV-$Cre^{(0/0)}/AR^{L-/Y}$ and CMV-$Cre^{(tg/0)}/AR^{L-/L-}$ mice. (*d*) Detection of the Y chromosome-specific *Sry* gene in $AR^{L-/Y}$ mice by PCR of mouse-tail DNA. (*e*) Lack of AR transcripts in male ($AR^{L-/Y}$) and female ($AR^{L-/L-}$) AR-null mutant mouse brains as shown by Northern blot analysis with an AR E-domain cDNA probe. (*f*) Absence of AR protein in $AR^{L-/Y}$ and $AR^{L-/L-}$ mouse brains by Western blot analysis with a specific C-terminal antibody. (*g*) Female-like external genitalia in $AR^{L-/Y}$ mice (*Upper*). Atrophic testis without internal male and female reproductive organs in $AR^{L-/Y}$ mice. Ep, epididymis; Pr, prostate; Sv, seminal vesicle; Te, testis; Vd, vas deferens; Od, oviduct, Ov, ovary; Ut, uterus.

clonal AR antibodies (C-19 and N-20; Santa Cruz Biotechnology) and then peroxidase-conjugated second antibody. Blots were visualized by using an ECL detection kit (Amersham Bioscience). Immunohistochemistry was performed as described in *Supporting Materials and Methods*.

Animal Conditions for Behavior Tests. Gonadally intact experimental mice (8 weeks old) were housed singly under controlled light (light/dark 12:12, lights off at 1800 hours) and temperature (22–24°C) conditions throughout the tests. For adult hormone administration, a Silastic tube [10 mm length, i.d. = 0.062 in (1 in = 2.54 cm), Dow–Corning] containing methyltrienolone (R1881; 5 mg/20 μl) (15), or 60-day time-release pellets (Innovative Research of America) containing either 5α-dihydrotestosterone (DHT; 10 mg per pellet), 17β-estradiol (E_2; 0.25 mg per pellet), or placebo (PLA) were implanted s.c. 2 weeks after gonadectomy under avertin anesthesia. All behavioral tests were conducted during the dark phase of the light/dark cycle, starting at 2 h after lights off.

Male Sexual Behavior Tests. Every week experimental mice underwent two 30-min sexual behavioral tests and then a 90-min test in their home cages (3, 4, 16). As stimuli, female mice (C57BL/6J) were ovariectomized and injected with estradiol benzoate (30 μg at 48 h and 15 μg at 24 h before tests) and progesterone (500 μg at 4 h before tests), with only females that showed lordosis in response to mounting by stud males subjected to experimentation. Sexual behaviors of each male were recorded for either 30 or 90 min as follows: number of mounts and intromissive and ejaculatory behaviors. The latency period (seconds) of the first male behavioral response was also measured.

Male Aggressive Behavior Test. Each mouse was tested three times in his home cage (as a resident) against an olfactory bulbectomized male (C57BL/6J) intruder mouse for 15 min (3, 4). For each experiment, percent of mice showing aggressive behaviors, total number of aggressive bouts, and latency (seconds) to first aggressive behavioral act by resident males were scored. An aggressive bout was defined as a consecutive series of behavioral acts separated by <3 sec, consisting of tail rattling, chasing, boxing, biting, offensive attacks, and wrestling.

Female Sexual Behavior Test. Gonadally intact or hormone-primed mice were introduced into a vigorous WT male's home cage (17). Lordosis in response to mount was defined as receptive posture with dorsoflexion of the back and elevation of the hindquarters. The lordosis quotient was calculated as the number of lordosis events per 10 mounts × 100. Observation continued for 20 min after introduction of the experimental animals, or until they received 10 mounts.

Perinatal DHT Treatment. Pregnant mice were implanted with 21-day time-release pellets (Innovative Research of America) containing DHT (35 mg per pellet) from days 14 to 19 of pregnancy. All offspring were injected with DHT (300 μg/30 μl) on days 0, 2, 4, 6, and 8 after birth. PLA and sesame oil were administered to control animals in the same schedule. These $AR^{L-/L-}$ and male and female WT mice were gonadectomized at 50 days of age, and behavioral tests were performed after hormone treatments as described above.

Statistical Analysis. Behavioral test data are shown as mean (±SE) and analyzed by using Student's t test or two-way ANOVA followed by post hoc comparison with the Fisher's protected least significant difference test. The nonparametric Kruskal–Wallis test and Mann–Whitney U test were used when variances were not equal among groups. Differences in incidences of behaviors were analyzed by the χ^2 test or Fisher's exact probability test.

Results

Generation of AR-Deficient Mice by Using the Cre-loxP System. To circumvent male infertility due to AR inactivation, we introduced three loxP sites around exon 1, which encodes the

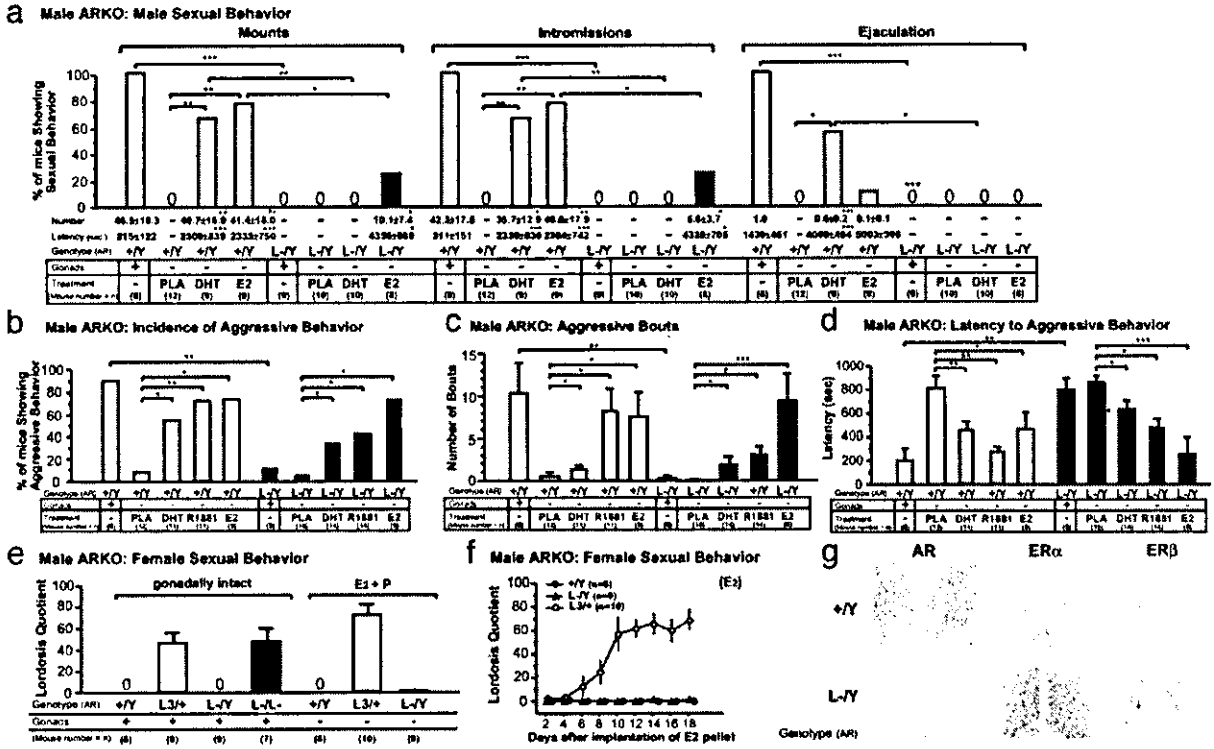

Fig. 2. Ablation of AR in male mice resulted in the lack of both male and female sexual behaviors. (*a*) Loss of all components of male sexual behavior in intact (gonads: +) 10-week-old $AR^{L-/Y}$ mice. E_2 treatment of gonadectomized (gonads: −) $AR^{L-/Y}$ mice partially induced mounts and intromissions but not ejaculation. Results of 90-min sexual behavioral tests performed after 30-min tests performed twice every week for 2 weeks are shown and were basically identical with those of the 30-min tests (data not shown). *, $P < 0.05$; **, $P < 0.01$; ***, $P < 0.001$. (*b*) Percentage of intact (gonads: +) and gonadectomized (gonads: −) 10-week-old mice exhibiting aggressive behaviors (Incidence of male aggressive behavior) toward olfactory bulbectomized (OBX) male intruder mice. Three tests in total were carried out every week, and results of the third test are shown. *, $P < 0.05$; **, $P < 0.01$. (*c*) Number of bouts with attacks. **, $P < 0.01$; ***, $P < 0.001$. (*d*) Latency to the first attack during resident–intruder tests. Aggressive behavioral acts were markedly reduced in intact $AR^{L-/Y}$ mice and were partially recovered after DHT treatment. *, $P < 0.05$; ***, $P < 0.001$. (*e*) Absence of female sexual behaviors in intact and E_2- and progesterone-primed gonadectomized 10-week-old $AR^{L-/Y}$ mice. Twenty days after implantation of E_2 pellets, progesterone (P; 500 μg) was administered to $AR^{L-/Y}$ and *WT* mice 4 h before the behavioral test. Normal expression of female sexual behaviors was observed in intact 10-week-old $AR^{L-/L-}$ mice. (*f*) Lordosis was not induced in gonadectomized $AR^{L-/Y}$ mice after treatment with E_2. (*g*) Absence of AR protein and no reduction in ERα and ERβ protein levels in the medial preoptic area of $AR^{L-/Y}$ mice analyzed by immunohistochemistry.

transcription start site (Fig. 1*a*), to generate *AR*-floxed (flox/Y) mice (Fig. 1*b*). *AR*-floxed male ($AR^{L3/Y}$) and female ($AR^{L3/+}$) mice exhibited no overt abnormalities in terms of sexual behaviors, with normal reproduction frequencies and AR mRNA expression levels (Fig. 1*e*). *AR*-floxed mice were then crossed with CMV-Cre transgenic mice (tg/0) to generate female AR heterozygotes ($AR^{L-/+}$) for further generation of male $AR^{L-/Y}$ and female $AR^{L-/L-}$ null mutant mice (Fig. 1*c*) as described (10). The genetic sex of male $AR^{L-/Y}$ and female $AR^{L-/L-}$ mice was confirmed by detection of the Y chromosome *Sry* gene (Fig. 1*d*). No AR transcripts in the brain were detected by Northern blotting (Fig. 1*e*), and RT-PCR using primer pairs designed to amplify exons encoding the *AR* ORF also failed to detect AR mRNA (data not shown). Immunoblotting experiments using N- and C-terminal antibodies for AR showed no AR protein expression in the brain and confirmed the inactivation of the *AR* gene (Fig. 1*f*).

Tfm Abnormalities in Male ARKO ($AR^{L-/Y}$) Mice. From birth, both $AR^{L-/Y}$ and $AR^{L-/L-}$ mice were externally indistinguishable from normal female WT littermates (Fig. 1*g*) in terms of anogenital distance ($AR^{L-/Y}$, 6.0 ± 0.6 mm; $AR^{L-/L-}$, 5.8 ± 0.5 mm; $AR^{+/Y}$, 16.2 ± 1.3 mm; and $AR^{L3/+}$, 5.9 ± 0.4 mm) and growth curve up to 10 weeks (Fig. 5*c*, which is published as supporting information on the PNAS web site). $AR^{L-/Y}$ mice exhibited female-typical external appearance, including a vagina with a blind end, and a clitoral-like phallus instead of a penis and scrotum (Fig. 1*g*), similar to that observed in another mice line (18). Male reproductive organs, including seminal vesicles, vas deferens, epididymis, and prostate, were absent in $AR^{L-/Y}$ mice (Fig. 1*g*). Although no ovaries or uteri were observed, small inguinal testes were present. Histological examination of these testes showed that spermatogenesis was severely arrested (Fig. 5*a*). Testicular androgen levels were very low [testosterone, $t(24) = 3.1$, $P < 0.01$; and DHT, $t(15) = 3.1$, $P < 0.01$], whereas serum estrogen levels appeared normal in 10-week-old mutant mice (Fig. 5*b*). To our surprise, no phenotypic abnormalities in female reproductive organs were found in female $AR^{L-/L-}$ mice up to 10 weeks of age (H. Shiina, J. Miyamoto, T. Sato, T. Matsumoto, and S. Kato, unpublished results).

Impaired Male-Typical Behaviors in ARKO Male Mice. On matching with WT stimulus females (3, 4, 16), gonadally intact 10-week-old $AR^{L-/Y}$ mice that had been housed singly exhibited no male sexual behaviors (Fig. 2*a*), including mounts [$\chi^2(1) = 17.0$, $P < 0.001$], intromissions [$\chi^2(1) = 17.0$, $P < 0.001$], and ejaculation [$\chi^2(1) = 17.0$, $P < 0.001$], despite having normal levels of serum E_2 (Fig. 5*b*) and normal levels of ER α and β protein expression in the hypothalamus (Fig. 2*g*). To restore the reduced serum androgen levels, gonadectomized $AR^{L-/Y}$ mice were given non-aromatizable androgen DHT. Although DHT treatment of WT male littermates enhanced the manifestation of male sexual

GENETICS

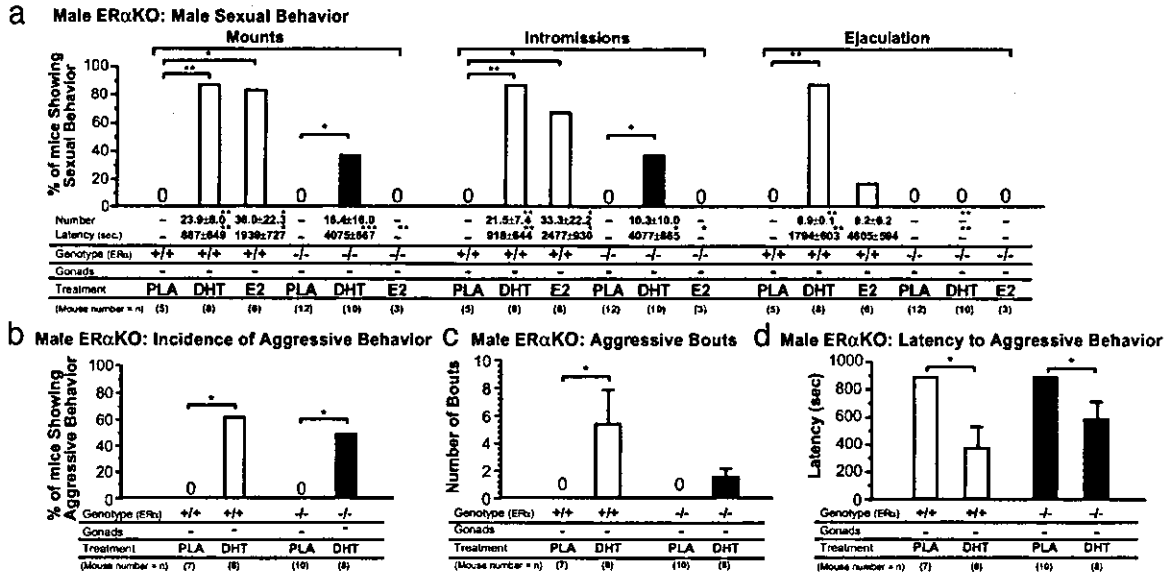

Fig. 3. Partial recovery of impaired male-typical behaviors in $ER\alpha^{-/-}$ mice after DHT treatment. (*a*) Treatment with DHT, but not E_2, restored the impaired mount and intromission but not ejaculation of gonadectomized 10-week-old male $ER\alpha^{-/-}$ mice. *, $P < 0.05$; **, $P < 0.01$; ***, $P < 0.001$. (*b*) Impaired male aggressive behaviors of male $ER\alpha^{-/-}$ mice were restored by DHT treatment. *, $P < 0.05$. (*c*) Number of bouts with attacks. *, $P < 0.05$. (*d*) Latency to the first attack during resident–intruder tests. *, $P < 0.05$.

behaviors [mounts and intromissions, $\chi^2(1) = 8.2, P < 0.01$, and ejaculation, $\chi 2(1) = 7.5, P < 0.05$], it was totally ineffective in $AR^{L-/Y}$ mice (Fig. 2*a*). Male aggressive behaviors (3, 4) were also severely impaired in $AR^{L-/Y}$ mice [$\chi^2(1) = 10.8, P < 0.01$] as measured by decreased numbers of aggressive bouts ($F_{7,79} = 6.71, P < 0.01$) with longer latency periods ($F_{7,79} = 6.55, P < 0.01$). Unexpectedly, treatment with either DHT or a nonaromatizable synthetic AR ligand (R1881) (15) enhanced, to at least some extent, the impaired male aggressive behaviors of $AR^{L-/Y}$ mice [DHT, $\chi 2(1) = 4.0, P < 0.05$, and R1881, $\chi 2(1) = 5.5, P < 0.05$; Fig. 2 *b–d*]. Our results suggested that both AR-independent and -dependent pathways mediated the effects of DHT on male aggressive behaviors.

In agreement with previous findings (2, 19), E_2 also potently induced male sexual behaviors in WT male mice [$\chi^2(1) = 10.5, P < 0.01$], whereas E_2-treated $AR^{L-/Y}$ mice showed recovery of mounts and intromissions [$\chi^2(1) = 5.2, P < 0.05$] but not ejaculation. However, where behavioral recovery did occur, it was only to ≈50% of that observed in WT mice (Fig. 2*a*). The impaired aggressive behaviors of male ARKO mice were effectively restored by E_2 treatment [$\chi^2(1) = 7.9, P < 0.01$; Fig. 2 *b–d*].

Absence of Female-Typical Behaviors in Male ARKO Mice. We then tested the female sexual behaviors of gonadally intact $AR^{L-/Y}$ mice by placing these mice into the home cages of WT males (17). $AR^{L-/Y}$ mice did not perform lordosis in response to WT male mounts (Fig. 2*e*). To further verify the inability of $AR^{L-/Y}$ mice to display lordosis, ovarian hormones were administered to stimulate female sexual behaviors. In WT females, the levels of lordosis gradually increased after administration of E_2, whereas no lordosis was induced in $AR^{L-/Y}$ mice even when progesterone was given together with E_2 (Fig. 2 *e* and *f*). In contrast, female intact $AR^{L-/L-}$ mice exhibited normal levels of lordosis, similar to that of WT females (Fig. 2*e*), and fertility (data not shown) but not male-typical behaviors.

Partial Recovery of Impaired Male-Typical Behaviors in $ER\alpha^{-/-}$ Mice after DHT Treatment. As male-typical behaviors have been shown to be impaired in male $ER\alpha^{-/-}$ mice (2, 4), but not in $ER\beta^{-/-}$ mice (2, 17), we attempted to verify the role of AR in male-typical behaviors by testing the effects of DHT in male $ER\alpha^{-/-}$ mice (20). In male WT mice, all three components of male sexual behaviors were enhanced after DHT treatment. In male $ER\alpha^{-/-}$ mice, DHT treatment restored impaired mount and intromission behaviors [$\chi 2(1) = 5.8, P < 0.05$], but not ejaculation (Fig. 3*a*). Similarly, the impaired aggressive behaviors of male $ER\alpha^{-/-}$ mice were partially recovered by DHT treatment as measured by increased incidences of aggression [$\chi^2(1) = 6.2, P < 0.05$] with shorter latencies ($F_{3,26} = 5.41, P < 0.05$; Fig. 3 *b–d*). Thus, male behavioral responses to DHT in null $ER\alpha^{-/-}$ mice further confirmed the physiological importance of androgen signaling in male-typical behaviors.

DHT-Induced Perinatal Brain Masculinization in Female Mice Was Abolished by AR Inactivation. Serum levels of testosterone in newborn $AR^{L-/Y}$ mice were still within the normal range compared with WT males (WT, 618.8 ± 233.1 pg/ml; and ARKO, 404.9 ± 171.7 pg/ml; Fig. 4*f*). However, we could not exclude the possibility that the lowered estrogen conversion due to impaired testosterone production from atrophic testis was insufficient to cause masculinization of the $AR^{L-/Y}$ fetal brain. Therefore, to precisely define the role of AR function in brain masculinization, we assessed AR-mediated androgen activity in the female fetus. Intact female brains physiologically undergo the innate feminization program due to the absence of sex hormone activity. It is well known that perinatal exposure of female rodents to androgens results in behavioral masculinization, observed as increased male-typical behavioral patterns after ovariectomy and further hormonal treatment in adulthood (5, 21). Only 30–33% of control WT females showed mount and intromissive patterns, but not ejaculatory patterns, even after either DHT or E_2 were administered in adulthood (Fig. 4*a*). In contrast, perinatal DHT treatment (see Fig. 6, which is published as supporting information on the PNAS web site) induced mount and intromissive patterns in WT females on further postpubertural DHT [mount and intromissions, $\chi^2(1) = 9.7, P < 0.01$] or E_2 [mount and intromissions, $\chi^2(1) = 10.5, P < 0.05$] treatment (Fig. 4*a*). Perinatal DHT exposure enabled 2 of 10 WT females to exhibit ejaculatory patterns in response to postpubertural DHT treatment. Similarly, male aggressive behaviors were also induced in

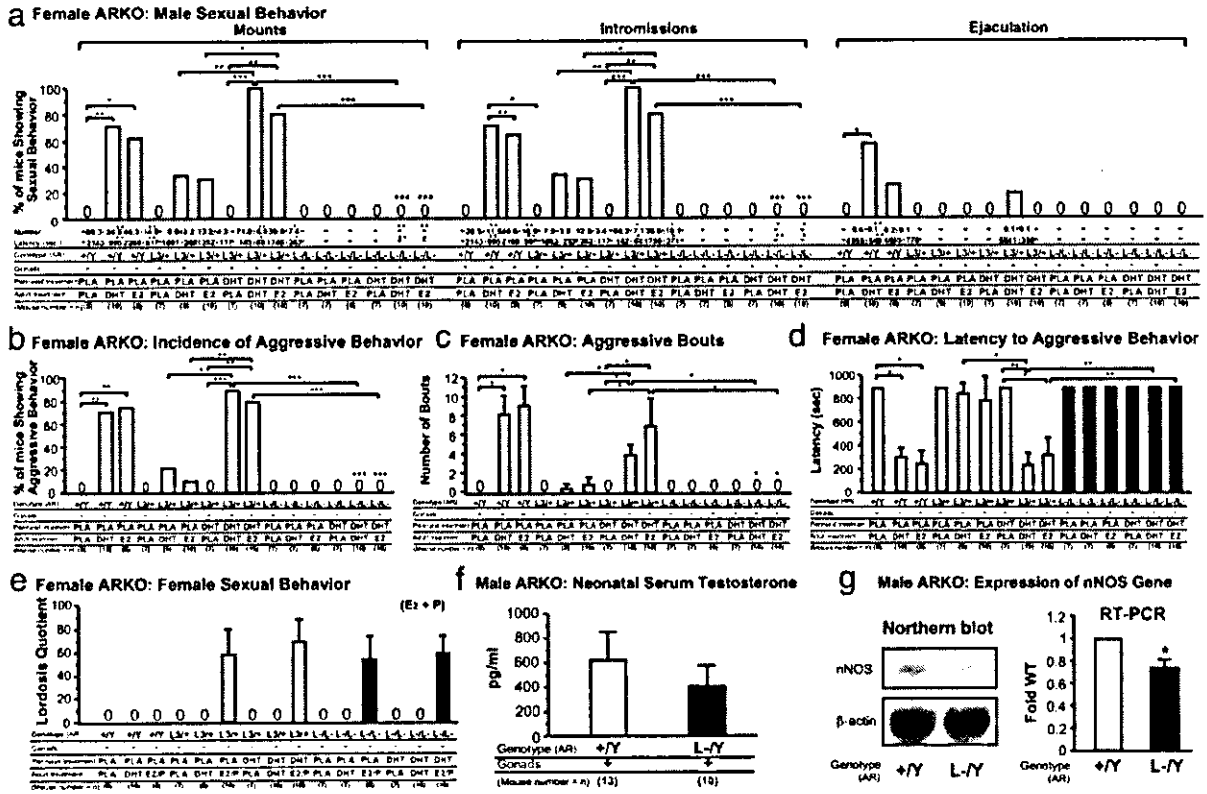

Fig. 4. Failure of $AR^{L-/L-}$ mice to express male-typical behaviors after DHT-induced perinatal brain masculinization. (*a*) WT female mice, but not $AR^{L-/L-}$ mice, showed male sexual behaviors in response to either DHT or E_2 treatment as adults after perinatal exposure to DHT. Behavioral tests were performed as described in Fig. 2*a*. *, $P < 0.05$; **, $P < 0.01$; ***, $P < 0.001$. (*b*) Percentage of mice exhibiting aggressive behaviors (incidence of male aggressive behavior) toward olfactory bulbectomized (OBX) male intruder mice. *, $P < 0.05$; **, $P < 0.01$; ***, $P < 0.001$. (*c*) Number of bouts with attacks. *, $P < 0.05$. (*d*) Latency to the first attack during resident–intruder tests. *, $P < 0.05$; **, $P < 0.01$. (*e*) Expression of female sexual behaviors is independent of AR/androgen signaling during the perinatal stage. Behavioral tests were performed after E_2 and progesterone treatment (E_2/P) as described in Fig. 2*e*. (*f*) No clear reduction in serum testosterone levels in $AR^{L-/Y}$ neonate mice (1 day after birth). (*g*) Reduced expression levels of nNOS transcript in $AR^{L-/Y}$ hypothalamus by Northern blot analysis. Densitometric analysis of the relative expression level by semiquantitative RT-PCR, expressed as fold WT after normalization to GAPDH. *, $P < 0.05$.

WT females exposed perinatally to DHT after either DHT [$\chi 2(1) = 6.5, P < 0.05$] or E_2 [$\chi 2(1) = 9.8, P < 0.01$] treatment in adulthood (Fig. 4 *b–d*). However, such male-typical patterns were completely abolished in female ARKO ($AR^{L-/L-}$) mice. Similar to control WT females, $AR^{L-/L-}$ mice exposed to perinatal DHT treatments exhibited normal female sexual behaviors in response to E_2 and progesterone (Fig. 4*e*). Thus, it is likely that full and normal brain masculinization and defeminization require both androgen and estrogen signaling.

Alteration in Gene Expression of Neuronal Nitric Oxide Synthase by AR Inactivation. Finally, to gain insight into the molecular basis of impaired male-typical behaviors in male ARKO mice, we analyzed the expression of several genes known to be involved in the control of male-typical behaviors (as described in *Supporting Results* in *Supporting Text*). No significant alterations in neuropeptide (oxytocin, vasopressin, and calcitonin gene-related peptide) and monoaminergic-specific gene [tyrosine hydroxylase, tryptophan hydroxylase, and 5-hydroxytryptamine (5-HT) receptor 5-HT1A and 5-HT1B] mRNA levels were detected by semiquantitative RT-PCR analysis of $AR^{L-/Y}$ mouse hypothalamus (Fig. 7 *a–g*, which is published as supporting information on the PNAS web site). In contrast, a clear reduction in nNOS mRNA expression in the hypothalamus of $AR^{L-/Y}$ mice was observed by Northern blotting and semiquantitative RT-PCR (Fig. 4*g*). Thus, our results suggested the possible involvement of NO neurotransmission in male-typical behaviors regulated by AR.

Discussion

The present study revealed that *AR* gene inactivation in intact male mice caused the complete loss of male sexual behaviors and severely reduced male aggressive behaviors. Furthermore, $AR^{L-/Y}$ mice displayed significantly reduced male-typical behaviors regardless of sex steroid hormone treatment. Thus, these results confirmed that AR function is critical for male-typical behaviors. Nevertheless, it was still impossible to determine whether impaired male-typical behavior in $AR^{L-/Y}$ mice was due to the lack of AR function in adulthood or the failure of masculinization because of AR deficiency during the perinatal stage.

To address this issue, we used female AR-null mutant mice and found that DHT-induced brain masculinization at the perinatal stage was abolished in $AR^{L-/L-}$ mice. These data provide genetic evidence that liganded-AR function alone is sufficient for the sexual conversion of perinatal female brains. Moreover, as both E_2- and DHT-induced male-typical behaviors in adult WT females treated perinatally with DHT, it is likely that once the brain is perinatally masculinized through activated AR function, the sexually developed brain becomes sensitive to both androgens and estrogens with regard to the expression of male-typical behaviors in adulthood. Thus, our results revealed that both brain masculinization during a limited perinatal period and expression of male-typical behaviors in adults require AR-mediated androgen signaling. Furthermore, the finding of significantly reduced nNOS mRNA levels after AR inactivation suggested that the nNOS gene may be one of the genes downstream of AR-mediated androgen signaling.

GENETICS

Male sexual behaviors were abolished in intact male ARKO mice, whereas treatment with E_2, but not DHT, rescued male sexual behaviors without the induction of female sexual behaviors. This finding indicated that the brains of $AR^{L-/Y}$ mice were defeminized and partially masculinized. However, human patients with severe Tfm are usually socially adopted as females, irrespective of castration and E_2 treatments. Together with the findings that prenatal treatment of female rhesus monkeys with DHT had clear and significant defeminizing and masculinizing effects on behavior (22), it appears that AR may serve a more critical role in male-typical behaviors than ER in higher mammals, including humans. Alternatively, because human sexuality is a complex behavioral trait formed through the combined function of multiple factors, the influence of social learning in humans might generate a species difference in terms of AR function in male sexual behaviors.

Examination of hormonal responses in $AR^{L-/Y}$ and $ER\alpha^{-/-}$ mice suggested that androgen and estrogen receptor functions are convergent with regard to male sexual behaviors. However, as ejaculation was not restored in single-receptor knockout mice by any of the hormone treatments, both AR and ER function appears to be essential for normal male sexual behaviors. Along with mapping the sites of receptor activity in the brain and identification of target genes, evaluation of the critical developmental stages for AR function and its downstream factors is of particular interest and will be greatly assisted by the spatiotemporal control of receptor gene inactivation (10).

Unlike male-typical behaviors, the expression of female sexual behaviors was unaffected by AR inactivation. Furthermore, perinatal DHT exposure had no effect on female sexual behaviors in $AR^{L-/L-}$ or WT female mice, and no female sexual behaviors were induced in $AR^{L-/Y}$ mice in response to any hormone treatment. These findings suggested that the defeminization process is totally independent from masculinization in the brains of both sexes and that the function of liganded ER, but not AR, appears to be indispensable for brain defeminization.

In contrast to male sexual behaviors, male aggressive behaviors appeared to be mediated at least in part by AR-independent signaling and were distinct from ER-mediated estrogen signaling. Although the molecular basis for this receptor-independent DHT action in males is unclear at present, DHT may exert its effects through an as-yet-unknown cell-membrane receptor (23). This hypothesis is supported by recent reports of the identification of cell membrane receptors for progesterone (24). Another possibility is that a currently unidentified DHT metabolite may be responsible for activating a nuclear receptor (25, 26) involved in male aggressive behaviors. Thus, AR-null mutant mice will be useful in further investigating novel androgen-signaling pathways that are independent of AR.

We thank G. K Schütz and K. S. Korach for helpful discussions, S. Aizawa for TT2 embryonic stem cells, J. Miyazaki for CAG-tester mice, and H. Higuchi and R. Nakamura for manuscript preparation. This work was supported in part by funding from the Human Frontier Science Program (to P.C. and S.K.) and a Grant-in-Aid for Priority Areas from the Ministry of Education, Science, Sports and Culture of Japan (to S.K.).

1. Couse, J. F. & Korach, K. S. (1999) *Endocr. Rev.* **20,** 358–417.
2. Ogawa, S., Chester, A. E., Hewitt, S. C., Walker, V. R., Gustafsson, J. A., Smithies, O., Korach, K. S. & Pfaff, D. W. (2000) *Proc. Natl. Acad. Sci. USA* **97,** 14737–14741.
3. Matsumoto, T., Honda, S. & Harada, N. (2003) *Neuroendocrinology* **77,** 416–424.
4. Ogawa, S., Lubahn, D. B., Korach, K. S. & Pfaff, D. W. (1997) *Proc. Natl. Acad. Sci. USA* **94,** 1476–1481.
5. Plapinger, L. & McEwen, B. S. (1978) in *Biological Determinants of Sexual Behaviour*, ed. Hutchison, J. B. (Wiley, New York).
6. Olsen, K. L. (1985) in *Neurobiology*, eds. Gilles, R. & Balthazart, J. (Springer, Heidelberg), pp. xv, 149–164.
7. Takeyama, K., Ito, S., Yamamoto, A., Tanimoto, H., Furutani, T., Kanuka, H., Miura, M., Tabata, T. & Kato, S. (2002) *Neuron* **35,** 855–864.
8. Quigley, C. A., De Bellis, A., Marschke, K. B., el-Awady, M. K., Wilson, E. M. & French, F. S. (1995) *Endocr. Rev.* **16,** 271–321.
9. Gaspar, M. L., Meo, T., Bourgarel, P., Guenet, J. L. & Tosi, M. (1991) *Proc. Natl. Acad. Sci. USA* **88,** 8606–8610.
10. Li, M., Indra, A. K., Warot, X., Brocard, J., Messaddeq, N., Kato, S., Metzger, D. & Chambon, P. (2000) *Nature* **407,** 633–636.
11. Sato, T., Matsumoto, T., Yamada, T., Watanabe, T., Kawano, H. & Kato, S. (2003) *Biochem. Biophys. Res. Commun.* **300,** 167–171.
12. Kato, S. (2002) *Clin. Pediatr. Endocrinol.* **11,** 1–7.
13. Ohtake, F., Takeyama, K., Matsumoto, T., Kitagawa, H., Yamamoto, Y., Nohara, K., Tohyama, C., Krust, A., Mimura, J., Chambon, P., *et al.* (2003) *Nature* **423,** 545–550.
14. Suzawa, M., Takada, I., Yanagisawa, J., Ohtake, F., Ogawa, S., Yamauchi, T., Kadowaki, T., Takeuchi, Y., Shibuya, H., Gotoh, Y., *et al.* (2003) *Nat. Cell Biol.* **5,** 224–230.
15. Cologer-Clifford, A., Simon, N. G., Richter, M. L., Smoluk, S. A. & Lu, S. (1999) *Physiol. Behav.* **65,** 823–828.
16. Matsumoto, T. & Yamanouchi, K. (2000) *Neurosci. Lett.* **291,** 143–146.
17. Ogawa, S., Chan, J., Chester, A. E., Gustafsson, J. A., Korach, K. S. & Pfaff, D. W. (1999) *Proc. Natl. Acad. Sci. USA* **96,** 12887–12892.
18. Yeh, S., Tsai, M. Y., Xu, Q., Mu, X. M., Lardy, H., Huang, K. E., Lin, H., Yeh, S. D., Altuwaijri, S., Zhou, X., *et al.* (2002) *Proc. Natl. Acad. Sci. USA* **99,** 13498–13503.
19. Meisel, R. L. & Sachs, B. D. (1994) in *The Physiology of Reproduction*, eds. Knobil, E. & Neill, J. D. (Raven, New York), pp. 3–105.
20. Dupont, S., Krust, A., Gansmuller, A., Dierich, A., Chambon, P. & Mark, M. (2000) *Development (Cambridge, U.K.)* **127,** 4277–4291.
21. Simon, N. G. & Whalen, R. E. (1987) *Horm. Behav.* **21,** 493–500.
22. Thornton, J. & Goy, R. W. (1986) *Horm. Behav.* **20,** 129–147.
23. Revelli, A., Massobrio, M. & Tesarik, J. (1998) *Endocr. Rev.* **19,** 3–17.
24. Zhu, Y., Rice, C. D., Pang, Y., Pace, M. & Thomas, P. (2003) *Proc. Natl. Acad. Sci. USA* **100,** 2231–2236.
25. Mangelsdorf, D. J., Thummel, C., Beato, M., Herrlich, P., Schutz, G., Umesono, K., Blumberg, B., Kastner, P., Mark, M., Chambon, P., *et al.* (1995) *Cell* **83,** 835–839.
26. Glass, C. K. & Rosenfeld, M. G. (2000) *Genes Dev.* **14,** 121–141.

THE JOURNAL OF BIOLOGICAL CHEMISTRY
Vol. 279, No. 34, Issue of August 20, pp. 35798–35802, 2004
Printed in U.S.A.

Disruption of Nuclear Vitamin D Receptor Gene Causes Enhanced Thrombogenicity in Mice*

Received for publication, May 3, 2004, and in revised form, June 16, 2004
Published, JBC Papers in Press, June 17, 2004, DOI 10.1074/jbc.M404865200

Ken-ichi Aihara‡§, Hiroyuki Azuma‡, Masashi Akaike‡, Yasumasa Ikeda‡, Michiko Yamashita¶, Toshiki Sudo‖, Hideki Hayashi‖, Yoshihisa Yamada‖, Fuminari Endoh, Mitsunori Fujimura‡, Tomonori Yoshida‡, Hiroshi Yamaguchi‡, Shunji Hashizume‡, Midori Kato‡, Kimihiro Yoshimura‡‡, Yoko Yamamoto‡‡, Shigeaki Kato‡‡, and Toshio Matsumoto‡**

*From the ‡Department of Medicine and Bioregulatory Sciences and the ¶Department of Pathology, University of Tokushima Graduate School of Medicine, 3-18-15 Kuramoto-cho, Tokushima 770-8503, the ‖First Institute of New Drug Discovery, Otsuka Pharmaceutical Co. Ltd., 463-10 Kagasuno, Kawauchi-cho, Tokushima 771-0192, the **Anatomic and Molecular Division, TSL, Inc., Higashimatuyama Laboratory, 656-1 Higashidaira Higashimatsuyama-shi, Saitama 355-0002, and the ‡‡Institute of Molecular and Cellular Biosciences, the University of Tokyo, 1-1-1 Yayoi, Bunkyo-ku, Tokyo 113-0032, Japan*

Vitamin D metabolites influence the expression of various genes involved in calcium homeostasis, cell differentiation, and regulation of the immune system. Expression of these genes is mediated by the activation of the nuclear vitamin D receptor (VDR). Previous studies have shown that a hormonally active form of vitamin D, 1α,25-dihydroxyvitamin D3, exerts anticoagulant effects in cultured monocytic cells. To clarify whether activation of VDR plays any antithrombotic actions *in vivo*, hemostatic/thrombogenic systems were examined in normocalcemic VDR knock-out (KO) mice on a high calcium diet and compared with wild type and hypocalcemic VDRKO mice that were fed a regular diet. Platelet aggregation was enhanced significantly in normocalcemic VDRKO mice compared with wild type and hypocalcemic VDRKO mice. Aortic endothelial nitric-oxide (NO) synthase expression and urinary NOx excretions were reduced in hypocalcemic VDRKO mice, but not in normocalcemic VDRKO mice. Northern blot and RT-PCR analyses revealed that the gene expression of antithrombin in the liver as well as that of thrombomodulin in the aorta, liver and kidney was down-regulated in hypo- and normocalcemic VDRKO mice. Whereas tissue factor mRNA expression in the liver and kidney was up-regulated in VDRKO mice regardless of plasma calcium level. Furthermore, VDRKO mice manifested an exacerbated multi-organ thrombus formation after exogenous lipopolysaccharide injection regardless of the calcemic conditions. These results demonstrate that activation of nuclear VDR elicits antithrombotic effects *in vivo*, and suggest that the VDR system may play a physiological role in the maintenance of antithrombotic homeostasis.

In many target organs, vitamin D exerts a variety of biological functions such as calcium homeostasis, cell proliferation, and cell differentiation. Most of these actions are exerted through the transcriptional control of target genes by the activation of the nuclear vitamin D receptor (VDR).[1] VDR is a ligand-inducible transcription factor that belongs to the nuclear receptor superfamily (1). VDR forms a heterodimer with the retinoid X receptor and binds to specific vitamin D-responsive elements on target genes (2, 3), which initiate sequences of events that lead to the activation or repression of target gene transcription by recruiting transcriptional cofactor complexes. Previous studies demonstrated that VDR knock-out (KO) mice manifest a variety of phenotypic abnormalities, including hypocalcemia, osteopenia, growth retardation, alopecia (4, 5), impaired immunity (6), hypertension with cardiac hypertrophy (7), and abnormal skeletal muscle development (8) and that most, but not all, of these phenotypic abnormalities can be rescued by normalization of serum mineral levels (6, 9).

In addition to its classical target tissues, VDR is also expressed in monocytic cells (10) and vascular endothelial cells (11), suggesting potential roles of vitamin D in antithrombotic functions. Koyama and colleagues (10, 12) have found that a hormonally active form of vitamin D, 1α,25-dihydroxyvitamin D3, as well as retinoic acid, exert anticoagulant effects by up-regulating the expression of the anticoagulant glycoprotein, thrombomodulin (TM), and by down-regulating the expression of a critical coagulation factor, tissue factor (TF), in cultured monocytic cells and human peripheral monocytes. However, it remains unclear whether activation of nuclear VDR can elicit antithrombotic actions *in vivo*. The present study was undertaken to clarify the physiological role of VDR-mediated actions in the hemostatic/thrombogenic system *in vivo*.

EXPERIMENTAL PROCEDURES

Animal Preparation—VDR homozygous mutants (4) and wild type (WT) control littermates were maintained as hybrids with C57BL/6J and CBA genetic backgrounds in a specific pathogen-free facility with a 12-h light and dark cycle. As reported previously (4, 9), a lactose-rich high calcium diet can normalize hypocalcemia in VDRKO mice, whereas a high calcium diet causes considerable hypercalcemia in WT mice. Therefore, after weaning (at 3 weeks of age) we divided the mice into three groups as follows: group 1 are WT mice fed a regular diet (containing 1.2% calcium and 1.0% phosphorus, Japan Clea, Tokyo, Japan); group 2 are VDRKO mice fed a regular diet (hypocalcemic); and

* This work was supported in part by Grants-in-aid for Priority Areas 830 and for Scientific Research 14370329 from the Ministry of Education, Science, Sports, and Culture of Japan. The costs of publication of this article were defrayed in part by the payment of page charges. This article must therefore be hereby marked "*advertisement*" in accordance with 18 U.S.C. Section 1734 solely to indicate this fact.

§ To whom correspondence should be addressed. Tel.: 81-88-633-7120; Fax: 81-88-633-7121; E-mail: aihara@clin.med.tokushima-u.ac.jp.

[1] The abbreviations used are: VDR, vitamin D receptor; AT, antithrombin; eNOS, endothelial nitric-oxide synthase; GFD, glomeruli with fibrin deposition; KO, knock-out; LPS, lipopolysaccharide; NO, nitric oxide; NOx, NO metabolites; PTH, parathyroid hormone; RARE, retinoic acid-responsive element; RT, reverse transcription; TF, tissue factor; TM, thrombomodulin; VDRE, vitamin D-responsive element; VDRKO, vitamin D receptor knock-out; WT, wild type.

group 3 are VDRKO mice fed a lactose-rich high calcium diet (normocalcemic). Experiments were conducted in 12-week-old mice that had been weaned then fed a specified diet for 9 weeks.

Blood Collection—Blood was collected from the inferior vena cava of mice under ether anesthesia. The blood was drawn with 21-gauge needles into plastic syringes containing 0.1 volume of 3.8% trisodium citrate solution. Some whole blood samples were used immediately for platelet aggregation analysis, and other whole blood samples were centrifuged at 2,000 × *g* for 10 min to obtain plasma. The plasma was stored at −80 °C until assayed.

Measurement of Plasma Calcium and Parathyroid (PTH) Hormone—Plasma levels of calcium and PTH were determined using the OCPC method and a rat PTH IRMA Kit (Immunotopics, Inc., San Clemente, CA), respectively.

Comparison of Platelet Aggregation with a Screen Filtration Pressure Method—Measurements of platelet aggregation with a screen filtration pressure aggregometer (WBA analyzer from SSR Engineering Co., Ltd., Yokohama, Japan) were performed according to a method described previously (13, 14). Reaction tubes containing 200-μl aliquots of whole blood were placed in an incubation chamber at 37 °C for 30 s followed by the addition of 22.2 μl of a serial concentration (1, 2, 4, 8 or 16 μM) of ADP (Sigma). 2 min after the addition of ADP, the blood samples were filtered through microsieve screens connected to a pressure sensor. A negative pressure of −130 mm Hg was established as 100%. The 0% pressure base line was established as −6 mm Hg, rather than 0 mm Hg because of the viscosity of whole blood. The platelet aggregation pressure of each reaction tube was determined as the pressure rate (percent). For the screen filtration pressure aggregometer study, the pressure rate was standardized using a grading curve produced by plotting four or five concentrations of ADP on the *x* axis and pressure rate (percent) on the *y* axis. The concentration of ADP causing a 50% increase in pressure rate was calculated and applied as the platelet aggregatory threshold index.

Measurement of Daily Urinary Excretion of Nitric Oxide Metabolites—To evaluate urinary excretion of nitric oxide (NO) metabolites (NOx), mice were housed individually in metabolic cages that provided free access to tap water and food for 24 h. NOx levels, from the murine urine, were determined by high performance liquid chromatography (15).

Estimation of Plasma Prothrombin Time and Activated Partial Thromboplastin Time—Plasma prothrombin time and activated partial thromboplastin time were determined by a scattered light detection method (16).

Measurement of Plasma Antithrombin (AT) Activity—Plasma AT activity was measured using N-test ATIII-S (Nittobo, Tokyo, Japan), which determines anticoagulant activity using a chromogenic substrate, according to the manufacturer's instructions.

Western Blot Analysis—Aortic tissue samples were homogenized in an ice-cold tissue protein extraction reagent (T-PER™, Pierce) containing protease inhibitors. Equal amounts of protein (50 μg) were loaded onto 10% acrylamide gels and then transferred to nitrocellulose membranes using a wet blot apparatus. Membranes were blocked overnight at 4 °C in blocking buffer (10 mM Tris-HCl, 10 mM NaCl, 0.1% polyoxyethylenesorbitan monolaurate) with 5% skim milk. The first antibody, mouse anti-human endothelial nitric-oxide synthase (eNOS) monoclonal antibody (1:1000 dilution, BD Transduction Laboratories, San Jose, CA), was applied for 1 h at room temperature. After a 30-min wash with the blocking buffer, membranes were probed with the second antibody (1:5000 dilution anti-mouse IgG horseradish peroxidase-linked whole antibody, Amersham Biosciences) for 1 h at room temperature. Membranes were washed again for 30 min. The membranes were then incubated with chemiluminescent reagents (ECL Western blotting Detection Reagents, Amersham Biosciences) for 5 min and then exposed to x-ray film. Band intensities were quantified using a NIH Image system.

RNA Isolation—Aortas, livers, and kidneys were rinsed with physiological saline. Total RNA was isolated by an acid guanidinium thiocyanate-phenol-chloroform extraction using TRIzol Reagent (Invitrogen). RNA concentrations were measured spectrophotometrically at 260 nm, and then samples were stored in diethyl dicarbonate-treated water at −80 °C.

Northern Blot Analysis—Approximately 20 μg of total RNA of the liver was fractionated on 1% formaldehyde-agarose gels and transferred to Hybond nylon membranes (Amersham Biosciences) by capillary action in a high salt solution (20 × SSC). Blots were prehybridized in a hybridization solution for 1 h at 42 °C followed by overnight hybridization with a digoxigenin-labeled specific oligonucleotide probe (DIG Northern Starter Kit, Roche Applied Science). Blots were washed twice in 2 × SSC and 0.1% SDS at room temperature for 5 min and then washed twice in 0.2 × SSC and 0.1% SDS at 68 °C for 15 min before exposure to x-ray film. The forward and reverse sequences of the AT oligonucleotide probe were: 5′-ATGATGTACCAGGAAGGCAA-3′ and 5′-GGAATGCGTCGGAGACATAG-3′, respectively. AT mRNA was estimated after correcting for loading differences by measuring the amount of 28 S rRNA.

RT-PCR Analysis—Expression of TF, TM, and glucose-3-phosphate dehydrogenase mRNA in aorta, liver, and kidney tissue were quantified by a RT-PCR method (8). Primers used were as follows: TF, forward 5′-CGGGTGCAGGCATTCCAGAG-3′ and reverse 5′-CTCCGTGGGACAGAGAGGAC-3′; TM, forward 5′-CAGGCTACCAGTTGGCTGCAG-3′ and reverse 5′-AGAGTTAGGGTCACAGTCTGC-3′; glucose-3-phosphate dehydrogenase; forward 5′-ACCACAGTCCATGCCATCAC-3′ and reverse 5′-TCCACCACCCTGTTGCTGTA-3′. PCR products were electrophoresed on 2.0% agarose gels, stained with ethidium bromide, visualized by ultraviolet transillumination, and photographed. Expression levels of TF and TM were expressed relative to the glucose-3-phosphate dehydrogenase signal.

Lipopolysaccharide-induced Thrombus Formation Experiments and Immunohistochemical Analysis—Mice were injected intraperitoneally with 5 mg/kg lipopolysaccharide (LPS) (*Escherichia coli* serotype 0111: B4; Sigma). 6 h later, mice were sacrificed, and lung, aorta, liver, and kidney tissue were removed. The tissue samples were placed immediately in 20% neutrally buffered formalin and stored overnight. After fixation, samples were embedded in paraffin, and 3-μm thick sections were produced. These tissue sections were deparaffinized, hydrated, and treated with a protease mixture (P-8038, Sigma) for 10 min at room temperature. After washing with deionized water, endogenous peroxidase was blocked with 3% hydrogen peroxide for 5 min, and then endogenous biotin was blocked with the DAKO Biotin Blocking System (DAKO Cytometion, Glostrup, Denmark). After washing with deionized water and blocking nonspecific staining by incubation with 10% porcine serum (GEMINI Bio-Products, Woodland, CA) in phosphate-buffered saline for 10 min at room temperature, the slides were incubated with rabbit anti-human fibrin-fibrinogen antibody (DAKO, 1:200 dilution) overnight at 4 °C. The slides were then rinsed with phosphate-buffered saline and incubated with (1:500) biotinylated $F(ab')_2$ fragments of swine anti-rabbit immunoglobulins (DAKO) for 30 min at room temperature. After rinsing with phosphate-buffered saline, the slides were incubated with diluted (1:500) peroxidase-conjugated streptavidin (DAKO) for 30 min at room temperature. Following incubation in 100 ml of phosphate-buffered saline containing 20 mg of 3,3′-diaminobenzidine tetrahydrochloride, 20 μl of 30% hydrogen peroxide, and 65 mg of sodium azide for 5 min at room temperature, the slides were counterstained with hematoxylin for 1 min. Finally, the sections were mounted after washing with deionized water and dehydration. The percentage of the glomeruli with fibrin deposition (% GFD) were calculated in all areas of each histological specimen of the kidney. Partially stained glomeruli were categorized as positive.

Statistical Analysis—Values for each parameter within a group were expressed as the mean ± S.E. For comparisons between genotypes, statistical significance was assessed using a one-way analysis of variance. Statistical significance was considered at $p < 0.05$.

RESULTS

Plasma Calcium and PTH Levels in WT and VDRKO Mice—The plasma calcium levels of VDRKO mice fed a regular diet were significantly low compared with WT mice (Fig. 1*A*). When VDRKO mice were fed a high calcium diet, plasma calcium levels were restored to levels similar to those in WT mice (Fig. 1*A*). As expected, marked elevation in plasma PTH levels were detected in VDRKO mice compared with WT mice. Consistent with the normalization of hypocalcemia from a high calcium diet (Fig. 1*B*), elevated plasma PTH levels decreased to similar levels observed in WT mice.

Aberrant Platelet Aggregation in VDRKO Mice—To examine the effect of VDR activation on platelet function, we first evaluated ADP-induced whole blood aggregation using a screen filtration pressure method in 12-week-old mice (Fig. 2*A*). Platelet aggregatory threshold index values in hypocalcemic VDRKO mice were increased markedly compared with those in WT mice ($p < 0.01$) (Fig. 2*B*). In contrast, platelet aggregatory threshold index values in normocalcemic VDRKO mice were significantly lower than those in WT mice ($p < 0.05$) (Fig. 2*B*).

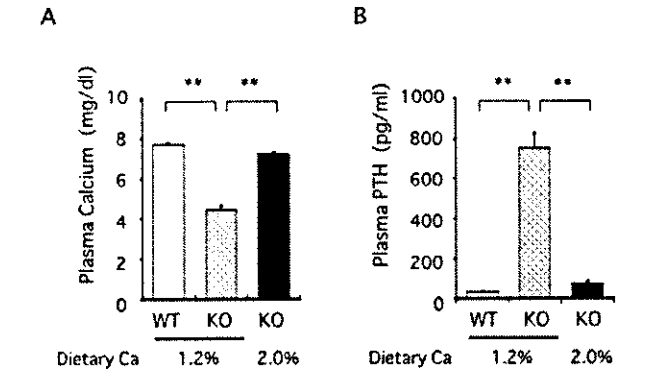

FIG. 1. **Plasma levels of calcium (*A*) and PTH (*B*) in WT mice and VDRKO mice at 12 weeks of age.** The number of mice examined in *A* and *B* was: 18 (WT, 1.2% calcium), 14 (KO, 1.2% calcium), and 14 (KO, 2.0% calcium). Values are expressed as the mean ± S.E. **, $p < 0.01$.

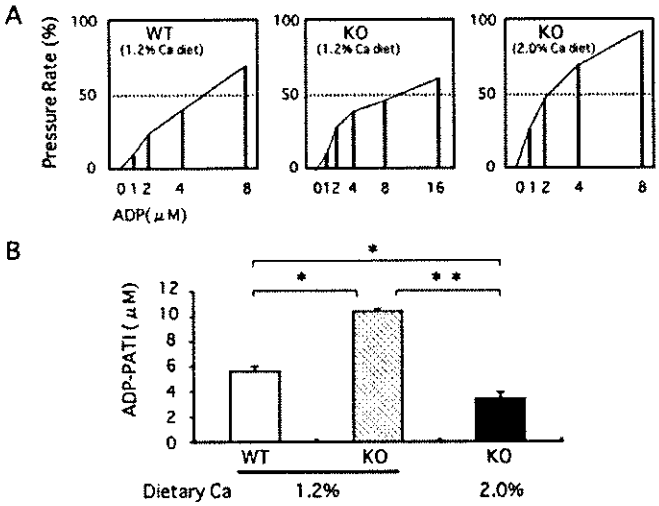

FIG. 2. **Representative results of platelet aggregation analyzed by the screen filtration pressure method in WT mice (1.2% calcium) and VDRKO mice (1.2% calcium, 2.0% calcium) at 12 weeks of age.** *A*, four or five different concentrations of agonist (ADP) were plotted along the *horizontal axis*, and their individual pressure rates (percent) were plotted along the *vertical axis*. *B*, the mean concentrations of agonist inducing a 50% pressure rate were calculated as the platelet aggregatory threshold index (*PATI*). The number of mice examined was: 14 (WT, 1.2% calcium), 10 (KO, 1.2% calcium), and 14 (KO, 2.0% calcium). Values are expressed as the mean ± S.E. *, $p < 0.05$, **, $p < 0.01$.

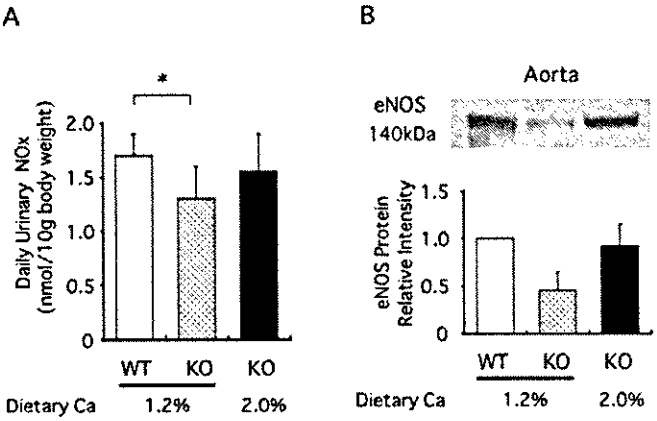

FIG. 3. *A*, daily urinary excretion levels of NOx in WT mice (1.2% calcium) and VDRKO mice (1.2% calcium, 2.0% calcium) at 12 weeks of age. The number of mice examined was: 18 (WT, 1.2% calcium), 14 (KO, 1.2% calcium), and 14 (KO, 2.0% calcium). Values are expressed as the mean ± S.E. *, $p < 0.05$. *B*, Western blot analysis of eNOS protein levels in the aorta. Protein levels of eNOS in aortic tissues of WT mice (1.2% calcium) and VDRKO mice (1.2% calcium, 2.0% calcium) at 12 weeks of age were determined by Western blot analysis and quantified densitometrically. Each *lane* contains 50 μg of protein. Six aortic tissues were examined in each group.

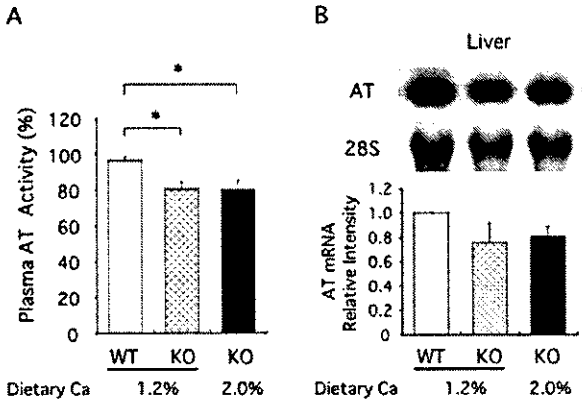

FIG. 4. *A*, plasma AT activity in WT mice (1.2% calcium) and VDRKO mice (1.2% calcium, 2.0% calcium) at 12 weeks of age. The number of mice examined was: 18 (WT, 1.2% calcium), 18 (KO, 1.2% calcium), and 16 (KO, 2.0% calcium). Values are expressed as the mean ± S.E. *, $p < 0.05$. *B*, Northern blot analysis of hepatic AT gene expression in WT mice (1.2% calcium) and VDRKO mice (1.2% calcium, 2.0% calcium) at 12 weeks of age. Six individual hepatic tissue samples were examined in each group. Values are expressed as the mean ± S.E.

These results demonstrate that hypocalcemia is responsible for the suppression of platelet aggregation in VDRKO mice fed a regular diet and that VDR itself has a suppressive effect on platelet aggregability.

Decreased Urinary Level of Nitric Oxide Metabolites in Hypocalcemic VDRKO Mice Was Restored by a High Calcium Diet—Because platelet aggregation is affected by the bioavailability of NO, we then analyzed urinary excretion of NOx (Fig. 3*A*). Daily urinary excretion of NOx in VDRKO mice was decreased significantly compared with WT mice. Feeding a high calcium diet (2.0% calcium) restored the urinary level of NOx in VDRKO mice to a level similar to that in WT mice. Thus, it is unlikely that the enhanced platelet aggregation in normocalcemic VDRKO mice is mediated by a change in NO level.

Impaired Aortic eNOS Expression in Hypocalcemic VDRKO Mice Was Normalized by High Calcium Diet—Western blot analysis demonstrated that eNOS protein levels in hypocalcemic VDRKO mice decreased to 45 ± 20% of WT mice. This may be a cause of decreased levels of urinary NOx excretion in hypocalcemic VDRKO mice (Fig. 3*B*). By feeding a high calcium diet, eNOS protein levels in VDRKO mice returned to levels similar to those in WT mice (Fig. 3*B*). These results indicate that reduced eNOS protein levels in VDRKO mice are mediated by hypocalcemia.

VDRKO Mice Manifested Normal Prothrombin Time and Activated Partial Thromboplastin Time—Although prothrombin time and activated partial thromboplastin time in WT, hypo-, and normocalcemic VDRKO mice were measured, no significant differences were noted among these mice in either prothrombin time (10.6 ± 0.4, 10.6 ± 0.2, 10.8 ± 0.6 s in WT, hypo-, and normocalcemic VDRKO mice, respectively) or activated partial thromboplastin time (58.0 ± 3.8, 54.5 ± 4.4, 56.4 ± 6.0 s in WT, hypo-, and normocalcemic VDRKO mice, respectively). These results demonstrate that the loss of VDR function does not lead to impaired blood coagulation and is consistent with the fact that VDRKO mice do not show a bleeding tendency.

Reduced Plasma Activity and Gene Expression of Antithrombin in VDRKO Mice—We next examined the plasma activity of

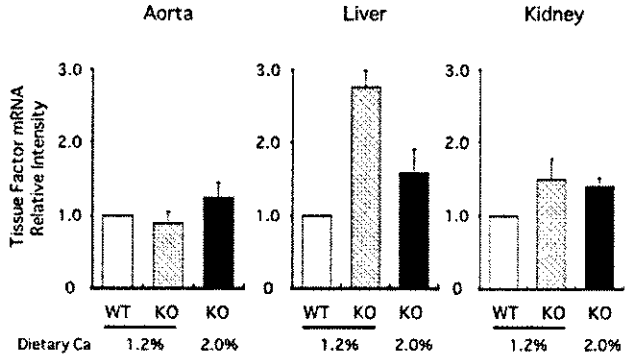

FIG. 5. **Quantitative analysis of TF mRNA levels in the aorta, liver, and kidney were performed by RT-PCR as described under "Experimental Procedures."** Total RNA was isolated from each organ of WT mice (1.2% calcium) and VDRKO mice (1.2% calcium, 2.0% calcium) at 12 weeks of age. Six individual tissue samples were examined in each group. Values are expressed as the mean ± S.E.

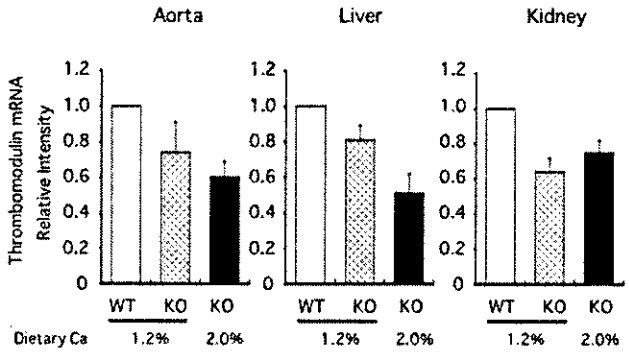

FIG. 6. **TM mRNA levels in the aorta, liver, and kidney were analyzed by RT-PCR as described under "Experimental Procedures."** Total RNA was isolated from each organ of WT mice (1.2% calcium) and VDRKO mice (1.2% calcium, 2.0% calcium) at 12 weeks of age. Six individual aorta, liver, and kidney tissue samples were examined in each group. Values are expressed as the mean ± S.E.

AT in these mice. Mean activities of plasma AT showed reductions in VDRKO mice regardless of their plasma calcium levels compared with those in WT mice (Fig. 4*A*). In addition, gene expression levels of AT in the liver were reduced by ~20% in both hypo- and normocalcemic VDRKO mice compared with those in WT mice (Fig. 4*B*). These results demonstrate that activated VDR positively regulates AT gene expression in the liver.

Aberrant Gene Expression of TF and TM in VDRKO Mice—As shown in Fig. 5, TF mRNA expression levels in the liver and kidney were enhanced in both hypo- and normocalcemic VDRKO mice compared with those in WT mice and tended to be higher in the aorta of normocalcemic VDRKO mice. In contrast, TM mRNA levels in the aorta, liver, and kidney were all reduced in VDRKO mice compared with those in WT mice (Fig. 6). Normalization of plasma calcium levels failed to correct the aberrant expression patterns of TF and TM genes in VDRKO mice (Figs. 5 and 6). These results indicate that activation of VDR elicits down-regulation of TF and up-regulation of TM gene expression, *in vivo*.

LPS-induced Thrombus Formation Was Exacerbated in VDRKO Mice—To test the possibility that the VDR system counteracts thrombotic stimuli, 5 mg/kg LPS was injected intraperitoneally to WT and VDRKO mice. All mice survived the treatment until sacrifice. Immunohistochemical analysis revealed that hypo- and normocalcemic VDRKO mice exhibited increased fibrin deposition in the glomeruli and peritubular capillaries of the kidney compared with WT mice (Fig. 7). Exacerbated fibrin deposition was also noted in the hepatic

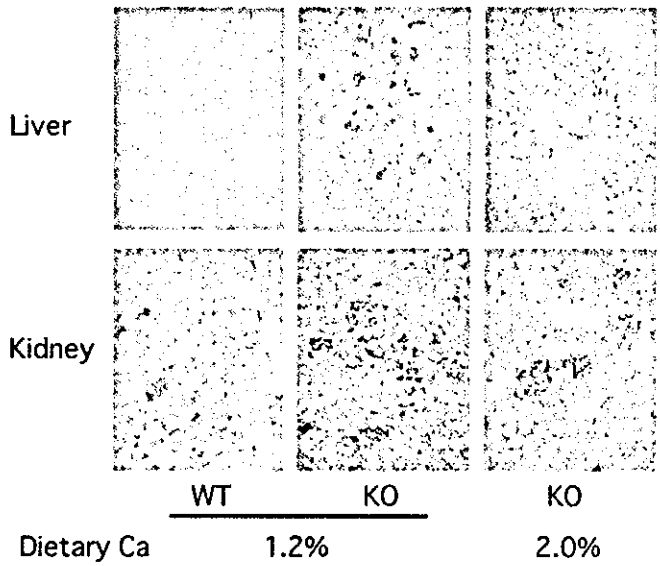

FIG. 7. **Immunohistochemical stainings with anti-fibrin-fibrinogen antibody of the liver (*upper panels*) and kidney (*lower panels*) after LPS injection, in WT mice (1.2% calcium) and VDRKO mice (1.2% calcium, 2.0% calcium) at 12 weeks of age.** Larger numbers of fibrin depositions were detected in both VDRKO mice compared with WT mice. Magnification, ×200.

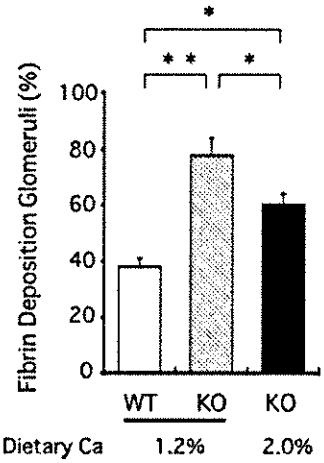

FIG. 8. **Percentage of glomeruli with fibrin deposition after LPS injection in WT mice (1.2% calcium) and VDRKO mice (1.2% calcium, 2.0% calcium) at 12 weeks of age.** LPS was injected intraperitoneally into mice as described under "Experimental Procedures." After 6 h, renal specimens were subjected to immunohistochemical analysis. The percentage of glomeruli with fibrin deposition was significantly higher in VDRKO mice than WT mice. Six individual renal tissue samples were examined in each group. Values are expressed as the mean ± S.E. *, $p < 0.05$, **, $p < 0.01$.

sinusoids of VDRKO mice regardless of plasma calcium levels (Fig. 7). No fibrin deposition was observed in the aorta or lung tissues from any group of mice (data not shown). To compare the degree of fibrin deposition quantitatively in the kidney, we compared the % GFD among three groups of mice. As shown in Fig. 8, the % GFD was significantly higher in both hypo- and normocalcemic VDRKO mice than that in WT mice. No fibrin deposition in the liver and kidney was observed when a vehicle was injected in both types of VDRKO mice (data not shown).

DISCUSSION

The present study demonstrates that ADP-induced platelet aggregation was enhanced significantly in normocalcemic VDRKO mice. Platelets are fragments of megakaryocytes that contribute to thrombus formation (17). Both normal hemostasis

and abnormal thrombosis depend on various regulatory factors within platelets (18). Physiological plasma calcium concentration is among the most important factors for normal platelet aggregation. Coordination of calcium flux through platelet-platelet contact serves to propagate calcium signaling throughout the developing thrombus to maintain thrombus growth (19). Thus, it is plausible to assume that the impaired platelet aggregation in hypocalcemic VDRKO mice was caused by the hypocalcemia in these mice. In contrast, molecular mechanisms underlying the accelerated platelet aggregation in normocalcemic VDRKO mice are unknown, and further investigations are required to understand VDR function in megakaryocytes and platelets.

There have been *in vitro* studies demonstrating that a hormonally active form of vitamin D up-regulates TM gene expression and down-regulates TF gene expression in monocytic cells (10, 12). However, *in vivo* effects of the vitamin D/VDR system on these factors have never been tested. In the present study, the gene expression of AT in the liver as well as that of TM in the aorta, liver, and kidney in VDRKO mice was down-regulated, whereas TF mRNA expression in the liver and kidney was up-regulated in VDRKO mice regardless of plasma calcium levels. Thus, the vitamin D/VDR system is shown to enhance the expression of antithrombotic factors while inhibiting the expression of a thrombogenic factor, TF.

AT is a plasma glycoprotein synthesized by hepatocytes and is one of the crucial inhibitors of blood coagulation through thrombin inactivation. Recently, AT-deficient mice were generated by gene targeting, and homozygous AT-null mice were shown to be prenatally lethal because of extensive thrombosis in the myocardium and liver sinusoids along with generally massive bleeding (20). In addition, heterozygous AT-deficient mice showed a tendency toward thrombus formation in the kidney after LPS injection (21). The present observations suggest that the vitamin D/VDR system may affect AT activity through transcriptional control of AT gene expression. Although Niessen *et al.* (22) reported ligand-dependent enhancement of human AT gene expression by retinoid X receptor α and thyroid hormone receptor β, their study revealed no effect of 1α,25-dihydroxyvitamin D3 on AT production. The reason why they were unable to observe the effect of the vitamin D/VDR system on AT gene transcription may be the use of a shortened AT gene promoter in their study (22).

Because all-*trans*-retinoic acid up-regulates TM expression in both monocytic and vascular endothelial cells via the retinoic acid-responsive element (RARE)-mediated transcriptional activation of the TM gene (10), and because RARE on the TM gene promoter is very similar to the vitamin D-responsive element (VDRE), there is a possibility that the effect of the vitamin D/VDR system on the up-regulation of TM gene expression is mediated via the binding of liganded VDR to the RARE of the TM gene (10, 12). In contrast, there is no evidence for transcriptional regulation of TF gene expression by the vitamin D/VDR system through VDRE or RARE. The TF gene promoter contains two activator protein-1 binding sites and a nuclear factor-κB site, and functional interactions between these two factors are required for maximal induction of TF gene transcription by tumor necrosis factor-α in vascular endothelial cells and by LPS in monocytic cells (23). Because interleukin-12 production from activated monocytic THP-1 cells is suppressed by 1α,25-dihydroxyvitamin D3 through the inhibition of nuclear factor-κB activation (24), the vitamin D/VDR system may suppress TF gene expression via modulation of nuclear factor-κB activation.

The present study also demonstrates that VDRKO mice manifest an exacerbated multiorgan thrombus after exogenous LPS injection regardless of the calcemic conditions. In agreement with the present results, Asakura *et al.* (25) demonstrated a beneficial effect of the active form of vitamin D3 against thrombosis, using a LPS-induced disseminated intravascular coagulation rat model. Enhanced platelet aggregation, down-regulated expression of AT and TM along with up-regulation of TF expression in both hypo- and normocalcemic VDRKO mice can all contribute to the enhanced thrombogenicity of VDRKO mice. In addition, deficiency of NO is associated with arterial thrombosis and thrombus formation in the renal vasculature of animal models and patients with endothelial dysfunction (26, 27). However, because reduced eNOS levels and urinary NOx excretion in hypocalcemic VDRKO mice were reversed in normocalcemic VDRKO mice, the exacerbated thrombus formation caused by LPS injection in normocalcemic VDRKO mice cannot be explained by a change in NO production. Although further investigation is needed to clarify the antithrombogenic effects of vitamin D3, the present results are consistent with the notion that the vitamin D/VDR system plays an important role in maintaining normal antithrombotic homeostasis *in vivo*.

Acknowledgment—We thank Geoff Falk for assistance in the preparation of the manuscript.

REFERENCES

1. Mangelsdorf, D. J., Thummel, C., Beato, M., Herrlich, P., Schutz, G., Umesono, K., Blumberg, B., Kastner, P., Mark, M., and Chambon, P. (1995) *Cell* **83,** 835–839
2. Haussler, M. R., Whitfield, G. K., Haussler, C. A., Hsieh, J. C., Thompson, P. D., Selznick, S. H., Dominguez, C. E., and Jurutka, P. W. (1998) *J. Bone Miner. Res.* **13,** 325–349
3. Takeyama, K., Masuhiro, Y., Fuse, H., Endoh, H., Murayama, A., Kitanaka, S., Suzawa, M., Yanagisawa, J., and Kato, S. (1999) *Mol. Cell. Biol.* **19,** 1049–1055
4. Yoshizawa, T., Handa, Y., Uematsu, Y., Takeda, S., Sekine, K., Yoshihara, Y., Kawakami, T., Arioka, K., Sato, H., Uchiyama, Y., Masushige, S., Fukamizu, A., Matsumoto, T., and Kato, S. (1997) *Nat. Genet.* **16,** 391–396
5. Li, Y. C., Pirro, A. E., Amling, M., Delling, G., Baron, R., Bronson, R., and Demay, M. B. (1997) *Proc. Natl. Acad. Sci. U. S. A.* **94,** 9831–9835
6. Mathieu, C., Van Etten, E., Gysemans, C., Decallonne, B., Kato, S., Laureys, J., Depovere, J., Valckx, D., Verstuyf, A., and Bouillon, R. (2001) *J. Bone Miner. Res.* **16,** 2057–2065
7. Li, Y. C., Kong, J., Wei, M., Chen, Z. F., Liu, S. Q., and Cao, L. P. (2002) *J. Clin. Invest.* **110,** 229–238
8. Endo, I., Inoue, D., Mitsui, T., Umaki, Y., Akaike, M., Yoshizawa, T., Kato, S., and Matsumoto, T. (2003) *Endocrinology* **144,** 5138–5144
9. Li, Y. C., Amling, M., Pirro, A. E., Priemel, M., Meuse, J., Baron, R., Delling, G., and Demay, M. B. (1998) *Endocrinology* **139,** 4391–4396
10. Koyama, T., Shibakura, M., Ohsawa, M., Kamiyama, R., and Hirosawa, S. (1998) *Blood* **92,** 160–167
11. Merke, J., Milde, P., Lewicka, S., Hugel, U., Klaus, G., Mangelsdorf, D. J., Haussler, M. R., Rauterberg, E. W., and Ritz, E. (1989) *J. Clin. Invest.* **83,** 1903–1915
12. Ohsawa, M., Koyama, T., Yamamoto, K., Hirosawa, S., Kamei, S., and Kamiyama, R. (2000) *Circulation* **102,** 2867–2872
13. Ozeki, Y., Sudo, T., Toga, K., Nagamura, Y., Ito, H., Ogawa, T., and Kimura, Y. (2001) *Thromb. Res.* **101,** 65–72
14. Sudo, T., Ito, H., and Kimura, Y. (2003) *Platelets* **14,** 239–246
15. Yamada, K., and Nabeshima, T. (1997) *J. Neurochem.* **68,** 1234–1243
16. Poller, L. (1988) *Thromb. Haemostasis* **60,** 18–20
17. Abrams, C., and Shattil, S. J. (1991) *Thromb. Haemostasis* **65,** 467–473
18. Nielsen, H. K. (1991) *Semin. Thromb. Hemostasis* **17,** (Suppl. 3) 250–253
19. Nesbitt, W. S., Giuliano, S., Kulkarni, S., Dopheide, S. M., Harper, I. S., and Jackson, S. P. (2003) *J. Cell Biol.* **160,** 1151–1161
20. Ishiguro, K., Kojima, T., Kadomatsu, K., Nakayama, Y., Takagi, A., Suzuki, M., Takeda, N., Ito, M., Yamamoto, K., Matsushita, T., Kusugami, K., Muramatsu, T., and Saito, H. (2000) *J. Clin. Invest.* **106,** 873–878
21. Yanada, M., Kojima, T., Ishiguro, K., Nakayama, Y., Yamamoto, K., Matsushita, T., Kadomatsu, K., Nishimura, M., Muramatsu, T., and Saito, H. (2002) *Blood* **99,** 2455–2458
22. Niessen, R. W., Rezaee, F., Reitsma, P. H., Peters, M., de Vijlder, J. J., and Sturk, A. (1996) *Biochem. J.* **318,** 263–270
23. Mackman, N. (1997) *Thromb. Haemostasis* **78,** 747–754
24. D'Ambrosio, D., Cippitelli, M., Cocciolo, M. G., Mazzeo, D., Di Lucia, P., Lang, R., Sinigaglia, F., and Panina-Bordignon, P. (1998) *J. Clin. Invest.* **101,** 252–262
25. Asakura, H., Aoshima, K., Suga, Y., Yamazaki, M., Morishita, E., Saito, M., Miyamoto, K., and Nakao, S. (2001) *Thromb. Haemostasis* **85,** 287–290
26. Loscalzo, J., Freedman, J., Inbal, A., Keaney, J. F., Jr., Michelson, A. D., and Vita, J. A. (2000) *Trans. Am. Clin. Climatol. Assoc.* **111,** 158–163
27. Verhagen, A. M., Rabelink, T. J., Braam, B., Opgenorth, T. J., Grone, H. J., Koomans, H. A., and Joles, J. A. (1998) *J. Am. Soc. Nephrol.* **9,** 755–762

Oncogene (2004) 23, 6000–6005

www.nature.com/onc

BRCA1 function mediates a TRAP/DRIP complex through direct interaction with TRAP220

Osamu Wada[1,2], Hajime Oishi[1,2], Ichiro Takada[1,3], Junn Yanagisawa[1,3], Tetsu Yano*[,1] and Shigeaki Kato[1,3]

[1]*Institute of Molecular and Cellular Biosciences, University of Tokyo, Yayoi 1-1-1, Bunkyo-ku, Tokyo 113-0034, Japan;* [2]*Department of Obstetrics and Gynecology, University of Tokyo, Hongo 7-3-1, Bunkyo-ku, Tokyo 113-8655, Japan;* [3]*SORST, Japan Science and Technology, Honcho 4-1-8, Kawaguchi, Saitama 332-0012, Japan*

Breast cancer susceptibility gene 1 (*BRCA1*) is a tumor suppressor gene mutated in a high percentage of hereditary breast and ovarian cancers. The multifunctional BRCA1 protein acts on cell cycle control, exerting several highly specialized DNA repair processes through diverse domains. Gene regulation through its C-terminal domain (BRCT) is indispensable for BRCA1-mediated tumor suppression, suggesting the possibility that the BRCT domain interacts with co-regulator complexes. Using a biochemical approach with HeLa S3 nuclear extracts, we isolated BRCT-associated complexes and identified one of the purified components as TRAP220. We then performed interaction studies *in vivo* (co-immunoprecipitation) and *in vitro* (glutathione S-transferase pull-down assays) and showed that BRCT directly interacted with TRAP220. This *in vitro* interaction was completely abolished by BRCT point mutations typical of those found in patients with BRCA1 that lack transactivation function. BRCA1 transactivation function was dependent on TRAP220 expression level in a transient expression assay. Moreover, a cell survival assay showed that antisense TRAP220 expression to disrupt endogenous TRAP220 expression significantly reduced the survival rate potentiated by BRCA1 after DNA damage. These results suggested that a TRAP220 complex play an important role as putative co-activator complexes in BRCA1-mediated tumor suppression.
Oncogene (2004) **23**, 6000–6005. doi:10.1038/sj.onc.1207786
Published online 21 June 2004

Keywords: BRCA1; TRAP220; breast cancer

Germ-line mutation of *BRCA1* is well known to predispose women to early onset of breast and ovarian cancer (Venkitaraman, 2002). The *BRCA1* gene encodes a relatively large protein of 1863 amino acids, and apart from an N-terminal zinc-binding RING domain and two C-terminal tandem copies of a BRCT motif, displays little similarity to other known proteins (Futreal *et al.*, 1994; Miki *et al.*, 1994). The C-terminal BRCT domain has been shown to be involved in double-stranded DNA repair and homologous recombination (Callebaut and Mornon, 1997; Moynahan *et al.*, 1999; Scully *et al.*, 1999; Zhong *et al.*, 1999). However, the major function of BRCT is thought to be as a gene regulator, mediating BRCA1 function as a tumor suppressor. This hypothesis is based on several lines of evidence, including that the autonomous transactivation function of BRCA1 was preserved in a recombinant protein consisting of the BRCT domain fused to a GAL4 DNA-binding domain (Miyake *et al.*, 2000). In addition, missense and point mutations in the BRCT domain derived from patients with inherited breast cancer result in the loss of transcriptional activity, and BRCA1 can also act as a negative regulator on some gene promoters (Chapman and Verma, 1996; Monteiro *et al.*, 1996; Zheng *et al.*, 2001; Kawai *et al.*, 2002). Reflecting the complex nature of BRCT transactivation function, this domain has already been shown to physically interact with a number of transcription factors and co-regulators (presumably in complexes), and also associate with chromatin remodeling complexes (Anderson *et al.*, 1998; Yu *et al.*, 1998; Zhang *et al.*, 1998; Yarden and Brody, 1999; Bochar *et al.*, 2000). Moreover, transcriptional squelching between BRCA1 and estrogen receptor (ER) has recently been reported (Fan *et al.*, 1999; Zheng *et al.*, 2001). As ER is a member of the nuclear receptor (NR) gene superfamily and acts as a ligand-induced transcription factor (Mangelsdorf *et al.*, 1995; Watanabe *et al.*, 2001; Yanagisawa *et al.*, 2002), limited cellular amounts of a common co-activator complex for both BRCA1 and ER could explain the transcriptional squelching phenomenon.

To better understand the BRCT transactivation function, we screened for putative transcription co-activator complexes that directly interacted with the BRCT domain using a biochemical approach. We established an affinity column whereby the BRCT domain (amino acids 1528–1863) was immobilized as a glutathione S-transferase (GST)-fusion protein. Fractions of HeLa S3 nuclear extract, presumably containing multiprotein complexes, were applied to the affinity

*Correspondence: T Yano;
E-mail: uskato@mail.ecc.u-tokyo.ac.jp
Received 8 October 2003; revised 24 March 2004; accepted 26 March 2004; published online 21 June 2004

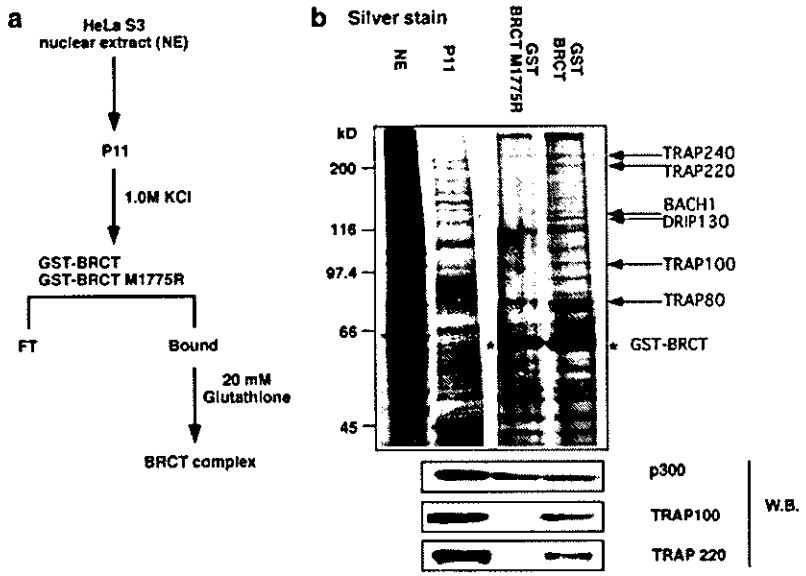

Figure 1 Affinity purification of BRCT-containing complexes (**a**) Purification scheme. HeLa S3 nuclear extract was fractionated using a phosphocellulose (P11) column and a GST-BRCT (amino acids 1528–1863) affinity column. The 1 M KCl P11 eluate was concentrated onto the GST-BRCT affinity column at 4°C for 10–12 h. Bound proteins were washed extensively with buffer, and subsequently eluted by buffer containing 20 mM reduced glutathione. As a negative control, purification from P11 eluates was performed using another affinity column (immobilized GST-BRCT M1775R). (**b**) Purified fractions were boiled, separated by electrophoresis and analysed by SDS–PAGE followed by silver staining or Western blot analysis using antibody, as shown on the right of the figure. Molecular weight standards are shown to the left of the figure. The asterisk denotes the molecular bait (GST-BRCT, GST-BRCT M1775R) after elution. Arrows show proteins identified by mass spectrometry (Yanagisawa *et al*., 2002)

column (Yanagisawa *et al*., 2002; Kitagawa *et al*., 2003), and several of the transcription co-regulators subsequently verified in the BRCT-interacting complexes by Western blotting (Figure 1b, lower panel). Western blotting of the BRCT-interacting complexes identified TRAP220 and TRAP100 (Figure 1b), which were confirmed as factors that associate with BRCT by time-of-flight mass spectrometry (TOF-MS). TRAP220 contains two LXXLL motifs, which are consensus interacting motifs and part of the core activation domain in NR ligand-binding domains (Fondell *et al*., 1999; Rachez *et al*., 1999). Thus, TRAP220 is thought to act as a major and direct interactant with ER (Yanagisawa *et al*., 2002), as well as with other NRs, as part of the common TRAP/DRIP co-activator complex (Rachez *et al*., 1999). It is therefore possible that the functional role of TRAP220 in the TRAP/DRIP complex may account for the reported transcriptional squelching between ER and BRCA1. Indeed, several other BRCT-associated proteins we identified were also TRAP/DRIP complex components, such as TRAP220, TRAP240, DRIP130, and TRAP80 (Ito *et al*., 1999). BACH1 (Cantor *et al*., 2001) and p300 (Pao *et al*., 2000) were also detected by TOF-MAS and Western blotting (Figure 1b), respectively, and have been previously shown to interact with BRCT, which confirmed the efficacy of our purification method.

To address the functional importance of the BRCT-TRAP220 interaction, a BRCT point-mutant, derived from a breast cancer patient and deficient in transcriptional activity, was used to isolate interacting complexes. As clearly shown in Figure 3b, the GST-fused BRCT point-mutant (M1775R) protein lacked the ability to retain TRAP220 on the column. This indicated that TRAP220 may function as a co-activator in the BRCA1 complex. To determine whether full-length BRCA1 protein interacted with TRAP220 in human cells, we expressed full-length BRCA1 (FLAG epitope-tagged) and/or TRAP220 (His/Myc epitope-tagged) in 293T cells. Significant expression of the tagged proteins was confirmed by Western blotting. After immunoprecipitation with anti-FLAG M2 to obtain full-length BRCA1, the immunoprecipitants were blotted with anti-Myc to identify TRAP220-containing complexes (Figure 2a). Both TRAP220 and BRCA1 were detected in cell lysate immunoprecipitates (Figure 2a), which supported the hypothesis that BRCA1 physically associates with TRAP220 in living cells. This hypothesis was further confirmed by *in vivo* association between endogenous BRCA1 and TRAP220 in MCF-7 cells expressing both proteins (Figure 2b). No such association was observed when the BRCA1 point-mutant (M1775R) was used instead of wild-type BRCA1 in the immunoprecipitation experiment (Figure 2a), as expected from the results of the column purification experiments.

To map the region of TRAP220 that interacted with BRCT, a GST pull-down assay was performed using TRAP220 deletion mutants (Figure 3a). FLAG-tagged TRAP220 fragments, abbreviated TR1, TR2, TR3, TR4 and TR5 (as described in Figure 3a), were *in vitro* translated in the presence of [^{35}S]methionine and incubated with GST-fused BRCT protein-bound resin. Only TR1 was trapped, which suggested that only the TR1 region interacted with BRCT. Interestingly, the

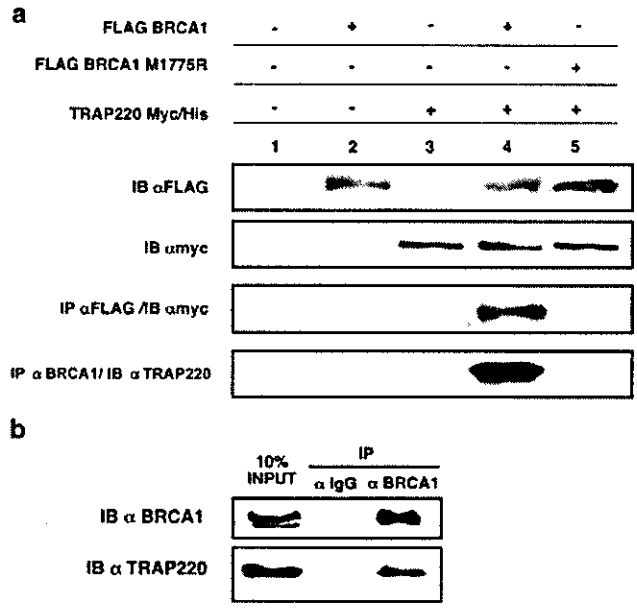

Figure 2 *In vivo* association between TRAP220 and BRCA1. (**a**) Formation of BRCA1 and TRAP220 complexes in 293T cells was analysed by co-immunoprecipitation (IP) using the anti-FLAG monoclonal M2 antibody (Sigma Aldrich) followed by immunoblotting (IB) using anti-Myc. 293T cells were transiently transfected with combinations of expression vectors as indicated. The expression of proteins in transfected cell extracts was determined by Western blot analysis using FLAG or Myc tags. (**b**) Detection of endogenous BRCA1-TRAP220 interaction by Western blotting. MCF-7 nuclear extracts were applied for immunoprecipitation with 5 μg of anti-BRCA1 (MS-BRC14-UP50, GeneTex, Inc.) and IgG, respectively. Then bound proteins in 30 μl of protein G sepharose™ 4 Fast Flow (Amersham Biosciences, NJ, USA) were detected by Western blotting. The 10% amount of the tested nuclear extracts is shown as positive control as input (Kitagawa *et al*., 2003)

BRCT column did not retain either TR2 or TR3, which contain LXXLL motifs thought to interact with liganded NRs. Reflecting the associations between TRAP220 and wild-type or point-mutant BRCA1 as observed in our *in vivo* experiments, the point-mutations A1708E, P1749R, and M1775R that exhibit no BRCA1 transactivation function caused the loss of TRAP220 interaction *in vitro* (Figure 3b).

To examine the co-activator activity of TRAP220 toward BRCT transactivation function, a transient transfection assay was performed using a luciferase reporter plasmid driven by the adenovirus major late promoter (AdMLP) containing GAL4DBD-binding sites. A BRCT-GAL4DBD-fusion protein (GAL-BRCT) alone potently stimulated transcription (Figure 4b). TRAP220 expression in human 293T cells led to an approximately twofold increase in luciferase activity compared to GAL-BRCT alone, while such co-activation was not detected in a TRAP220 deletion mutant lacking the BRCT interacting TR1 region (amino acids 1–326, see Figure 3a) (Figure 4b). This enhancement of transactivation by TRAP220 was not observed when either GAL4 DNA-binding domain alone or GAL-BRCT mutants (A1708E, P1749R, or M1775R) were used, as expected from the *in vivo* and *in vitro* TRAP220 experiments. Consistent with these findings, antisense TRAP220 expression, that disrupted endogenous TRAP220 expression (Figure 4a), reduced the transcriptional activity of BRCT (Figure 4b). This again suggested a significant role for TRAP220 in BRCA1 transactivation function.

Finally, we then tested the significance of TRAP220 activity in the DNA damage response mediated by BRCA1. BRCA1 was transfected into HCC1937 cells (a

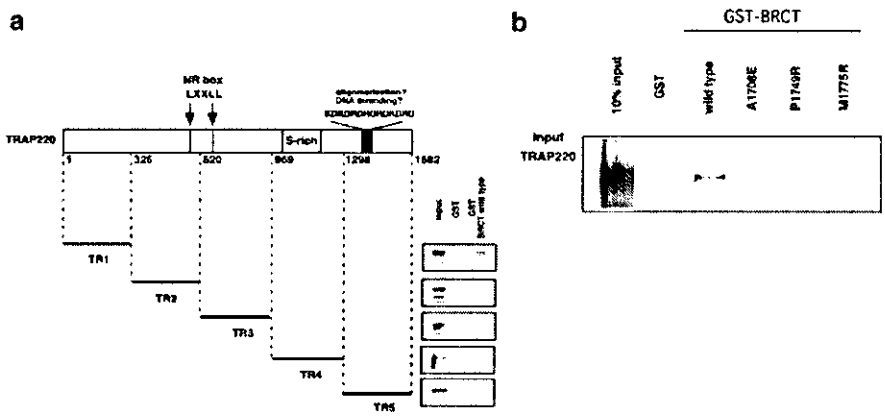

Figure 3 *In vitro* association between TRAP220 and BRCT, and mapping of the BRCT-interacting region of TRAP220. (**a**) Mapping of the BRCT-interacting region of TRAP220 using GST-BRCT and TRAP220 fragments. Bacterially expressed GST-fusion proteins immobilized on beads were used in *in vitro* pull-down assays. A schematic diagram of the structure of TRAP220 is shown. TRAP220 'TR1' (amino acids 1–326), 'TR2' (326–620), 'TR3' (620–969), 'TR4' (969–1298), and 'TR5' (1298–1582) were *in vitro* translated in the presence of [^{35}S]methionine (Amersham Pharmacia Biotech) using a TNT coupled *in vitro* translation system (Promega). Each labelled TRAP220 fragment was then incubated with either GST alone or GST-BRCT. The mixtures were washed and subjected to SDS–PAGE and analysed. Polyacrylamide gels were stained briefly with Coomassie Brilliant Blue to verify the loading of equal amounts of fusion proteins prior to drying and autoradiography (Ohtake *et al*., 2003). (**b**) *In vitro* association of TRAP220 with BRCT or BRCT point mutants that lack transcriptional activity were performed by incubating GST, GST-BRCT, GST-BRCT A1708E, P1749R, or M1775R with *in vitro* translated TRAP220

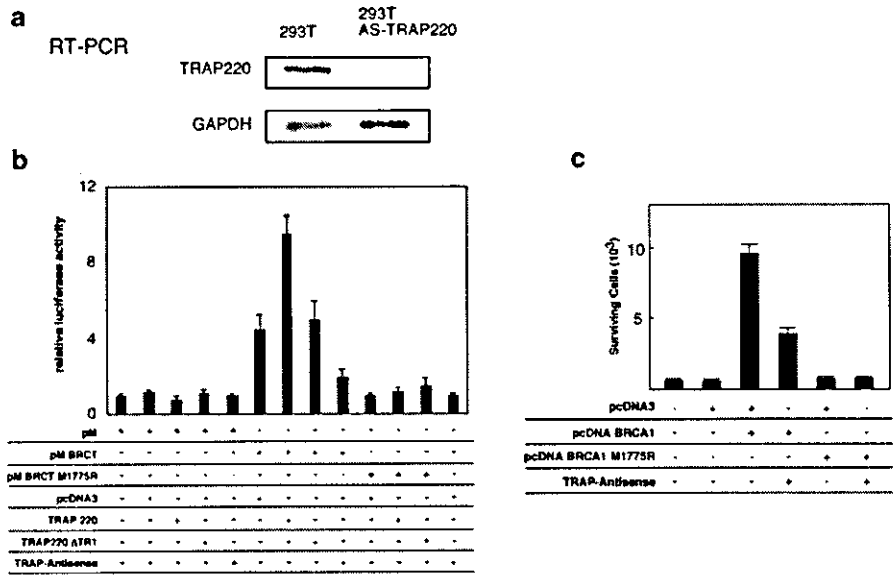

Figure 4 TRAP220 activates transcription by GAL-BRCT, while antisense TRAP220 disrupts the DNA damage response of BRCA1. (a) Transfection of antisense TRAP220 in 293T cells reduced TRAP220 expression as shown by RT-PCR analysis. (b) Transient transfection assays of GAL-BRCT and FLAG-TRAP220 using a luciferase reporter (Promega) containing the GAL4 DNA-binding site (17M8) showed specific enhancement of transcription. 293T cells were transfected with each luciferase reporter (E1b-Luc and AdMLP-Luc), pM or pM-BRCT, pRL CMV-Luc as a control of transfection efficiency, and either pcDNA3 (Invitrogen) empty expression vector, pcDNA FLAG-TRAP220, pcDNA TRAP220ΔTR1 or antisense TRAP220. Measurements of luciferase (Promega) activity were performed according to the manufacturer's instructions. Error bars indicate the standard deviation. Each experiment was repeated at least three times in triplicate (Watanabe *et al.*, 2001). (c) HCC1937 cells were transfected with constructs based on the pcDNA3 plasmid. Cultures were treated with 0.1% MMS for 50 min, and surviving cells were counted after 8 days, as previously described by Zhong *et al.* (1999)

mutated BRCA1 cell line) that are hypersensitive to DNA damaging agents such as methylmethane sulfonate (MMS). By counting the number of surviving HCC1937 cells, we observed a protective effect of BRCA1 expression in response to DNA damage. Antisense TRAP220 expression resulted in specific deterioration in the DNA damage response potentiated by BRCA1 (Figure 4c), which verified the importance of TRAP220 in BRCA1 function.

BRCA1 is a multifunctional protein that acts as a tumor suppressor controlling gene expression, as well as a sequence-specific regulator and a co-regulator controlling DNA damage (Venkitaraman, 2002). Therefore, it can be speculated that BRCA1 acts as a platform protein that associates with a number of factors, regulators, and complexes to accomplish the diverse functions attributed to BRCA1. Indeed, discrete classes of factors and complexes involved in gene regulation and DNA repair associated with BRCA1 have been identified, and indirect associations with further related factors and complexes are supposed. Nevertheless, clear relationships between *BRCA1* gene mutation and consequent malfunctions of the identified factors and complexes remain to be established. To this end, we searched for co-activator complexes that recognized the BRCT domain, as mutations in this domain modulate BRCA1 transactivation function and are highly related with breast and ovarian cancer incidence (Humphrey *et al.*, 1997; Greenman *et al.*, 1998). Also, a previous report found that BRCA1 competed with ER in terms of transcriptional control via the BRCT domain, which suggested the possibility of common co-activator complexes between ER and BRCA1, presumably including the TRAP/DRIP complex already identified as an ER co-activator complex (Ito *et al.*, 1999; Rachez *et al.*, 1999; Yanagisawa *et al.*, 2002).

In this study based on biochemical approaches (Yanagisawa *et al.*, 2002; Kitagawa *et al.*, 2003), we showed that a TRAP220-containing complex associated with wild-type BRCT through physical interaction with TRAP220. As TRAP220 binding of BRCA1 was abrogated *in vivo* and *in vitro* when clinically relevant BRCA1 mutants that lacked transactivation function (Chapman and Verma, 1996) were used as bait, the association between BRCT and TRAP220 complexes appears to be critical for normal BRCA1 function. This is supported by the findings that TRAP220 alone potently enhanced BRCA1 transactivation function, and that the disruption of endogenous TRAP220 by antisense TRAP220 led to a clear reduction in BRCA1-mediated DNA damage repair. This last result suggested that TRAP220-containing complexes may also play a role in the DNA damage repair function of BRCA1.

The TRAP/DRIP mediator complex was originally isolated as a co-activator complex for different classes of activators, including NRs, by several independent groups (Fondell *et al.*, 1996; Rachez *et al.*, 1999). Further study of the isolated complex components

revealed that the complexes formed a class of co-activator complexes that shared common major components along with limited numbers of specific factors (Gu *et al*., 1999). Combinations of these specific components generate a number of TRAP/DRIP complex subclasses (Freedman, 1999). The co-activator function of TRAP/DRIP complexes in *in vitro* transcription systems illustrates the direct link of the activator complex to the basal transcription machinery. The 220-kDa component of the complex, referred to as TRAP220/DRIP230, was identified as a subunit with unique properties in that it directly binds to NRs in a ligand-dependent manner through a region containing NR recognition motifs (LXXLL, NR box) (Ito *et al*., 1999; Rachez *et al*., 1999). Given that BRCA1 may compete with ER with respect to gene regulation, and that mutations in the BRCT region lead altered BRCA1-dependent gene regulation and enhanced tumorigenesis in estrogen-dependent cancers (presumably through modulation of ER-mediated estrogen signaling), interaction between TRAP220 and BRCA1 may account for the transcriptional squelching observed between BRCA1 and ER (Fan *et al*., 1999; Zheng *et al*., 2001).

The results of our study showed that TRAP220 bound directly to wild-type BRCA1, but not to BRCA1 mutants. Thus, breast cancer predisposition caused by genetic mutations in the BRCT domain may be due, at least in part, to insufficient interaction with TRAP complexes. In this respect, it is perhaps surprising that gene amplification or overexpression of TRAP220 is observed in some cancer cell lines (Zhu *et al*., 1999). Our transient transfection assay showed that TRAP220 enhanced BRCT-mediated transactivation function, such that the TRAP complex clearly served as a co-activator complex in the promoters of BRCA1 target genes. In conclusion, we propose that the failure of binding between BRCT and TRAP220 is a key event in cancer predisposition. Further investigations should be performed to elucidate the molecular mechanisms that underlie the formation BRCA1-TRAP complexes in normal cell growth, thereby revealing its role as a tumor suppressor in estrogen-responsive organs, especially the breast and ovary.

Abbreviations

BRCA1, breast cancer susceptibility gene 1; GST, glutathione S-transferase; CMV, cytomegalovirus; AdMLP, adenovirus major late promoter; NR, nuclear receptor.

Acknowledgements

We thank H Kitagawa and S Takezawa for helpful discussion and H Higuchi for manuscript preparation. This work was supported in part by grants-in-aid for priority areas from the Ministry of Education, Science, Sports, and Culture of Japan (to SK).

References

Anderson SF, Schlegel BP, Nakajima T, Wolpin ES and Parvin JD. (1998). *Nat. Genet.*, **19**, 254–256.

Bochar DA, Wang L, Beniya H, Kinev A, Xue Y, Lane WS, Wang W, Kashanchi F and Shiekhattar R. (2000). *Cell*, **102**, 257–265.

Callebaut I and Mornon JP. (1997). *FEBS Lett.*, **400**, 25–30.

Cantor SB, Bell DW, Ganesan S, Kass EM, Drapkin R, Grossman S, Wahrer DC, Sgroi DC, Lane WS, Haber DA and Livingston DM. (2001). *Cell*, **105**, 149–160.

Chapman MS and Verma IM. (1996). *Nature*, **382**, 678–679.

Fan S, Wang J, Yuan R, Ma Y, Meng Q, Erdos MR, Pestell RG, Yuan F, Auborn KJ, Goldberg ID and Rosen EM. (1999). *Science*, **284**, 1354–1356.

Fondell JD, Ge H and Roeder RG. (1996). *Proc. Natl. Acad. Sci. USA*, **93**, 8329–8333.

Fondell JD, Guermah M, Malik S and Roeder RG. (1999). *Proc. Natl. Acad. Sci. USA*, **96**, 1959–1964.

Freedman LP. (1999). *Cell*, **97**, 5–8.

Futreal PA, Liu Q, Shattuck-Eidens D, Cochran C, Harshman K, Tavtigian S, Bennett LM, Haugen-Strano A, Swensen J, Miki Y, Eddington K, McClure M, Frye C, Weaver-Feldhaus J, Ding W, Gholami Z, Söderkrist P, Terry L, Jhanwar S, Berchuck A, Iglehart JD, Marks J, Ballinger DG, Barrett JC, Skolnick MH, Kamb A and Wiseman R. (1994). *Science*, **266**, 120–122.

Greenman J, Mohammed S, Ellis D, Watts S, Scott G, Izatt L, Barnes D, Solomon E, Hodgson S and Mathew C. (1998). *Genes Chromosomes Cancer*, **21**, 244–249.

Gu W, Malik S, Ito M, Yuan CX, Fondell JD, Zhang X, Martinez E, Qin J and Roeder RG. (1999). *Mol. Cell.*, **3**, 97–108.

Humphrey JS, Salim A, Erdos MR, Collins FS, Brody LC and Klausner RD. (1997). *Proc. Natl. Acad. Sci. USA*, **94**, 5820–5825.

Ito M, Yuan CX, Malik S, Gu W, Fondell JD, Yamamura S, Fu ZY, Zhang X, Qin J and Roeder RG. (1999). *Mol. Cell.*, **3**, 361–370.

Kawai H, Li H, Chun P, Avraham S and Avraham HK. (2002). *Oncogene*, **21**, 7730–7739.

Kitagawa H, Fujiki R, Yoshimura K, Mezaki Y, Uematsu Y, Matsui D, Ogawa S, Unno K, Okubo M, Tokita A, Nakagawa T, Ito T, Ishimi Y, Nagasawa H, Matsumoto T, Yanagisawa J and Kato S. (2003). *Cell*, **113**, 905–917.

Mangelsdorf DJ, Thummel C, Beato M, Herrlich P, Schutz G, Umesono K, Blumberg B, Kastner P, Mark M, Chambon P and Evans RM. (1995). *Cell*, **83**, 835–839.

Miki Y, Swensen J, Shattuck-Eidens D, Futreal PA, Harshman K, Tavtigian S, Liu Q, Cochran C, Bennett LM, Ding W, Bell R, Rosenthal J, Hussey C, Tran T, McClure M, Frye C, Hattier T, Phelps R, Haugen-Strano A, Katcher H, Yakumo K, Gholami Z, Shaffer D, Stone S, Bayer S, Wray C, Bogden R, Dayananth P, Ward J, Tonin P, Narod S, Bristow PK, Norris FH, Helvering L, Morrison P, Rosteck P, Lai M, Barrett JC, Lewis C, Neuhausen S, Cannon-Albright L, Goldgar D, Wiseman R, Kamb A and Skolnick MH. (1994). *Science*, **266**, 66–71.

Miyake T, Hu YF, Yu DS and Li R. (2000). *J. Biol. Chem.*, **275**, 40169–40173.

Monteiro AN, August A and Hanafusa H. (1996). *Proc. Natl. Acad. Sci. USA*, **93**, 13595–13599.

Moynahan ME, Chiu JW, Koller BH and Jasin M. (1999). *Mol. Cell.*, **4**, 511–518.

Ohtake F, Takeyama K, Matsumoto T, Kitagawa H, Yamamoto Y, Nohara K, Tohyama C, Krust A, Mimura J, Chambon P, Yanagisawa J, Fujii-Kuriyama Y and Kato S. (2003). *Nature*, **423**, 545–550.

Pao GM, Janknecht R, Ruffner H, Hunter T and Verma IM. (2000). *Proc. Natl. Acad. Sci. USA*, **97**, 1020–1025.

Rachez C, Lemon BD, Suldan Z, Bromleigh V, Gamble M, Naar AM, Erdjument-Bromage H, Tempst P and Freedman LP. (1999). *Nature*, **398**, 824–828.

Scully R, Ganesan S, Vlasakova K, Chen J, Socolovsky M and Livingston DM. (1999). *Mol. Cell.*, **4**, 1093–1099.

Venkitaraman AR. (2002). *Cell*, **108**, 171–182.

Watanabe M, Yanagisawa J, Kitagawa H, Takeyama K, Ogawa S, Arao Y, Suzawa M, Kobayashi Y, Yano T, Yoshikawa H, Masuhiro Y and Kato S. (2001). *EMBO J.*, **20**, 1341–1352.

Yanagisawa J, Kitagawa H, Yanagida M, Wada O, Ogawa S, Nakagomi M, Oishi H, Yamamoto Y, Nagasawa H, McMahon SB, Cole MD, Tora L, Takahashi N and Kato S. (2002). *Mol. Cell.*, **9**, 553–562.

Yarden RI and Brody LC. (1999). *Proc. Natl. Acad. Sci. USA*, **96**, 4983–4988.

Yu X, Wu LC, Bowcock AM, Aronheim A and Baer R. (1998). *J. Biol. Chem.*, **273**, 25388–25392.

Zhang H, Somasundaram K, Peng Y, Tian H, Bi D, Weber BL and El-Deiry WS. (1998). *Oncogene*, **16**, 1713–1721.

Zheng L, Annab LA, Afshari CA, Lee WH and Boyer TG. (2001). *Proc. Natl. Acad. Sci. USA*, **98**, 9587–9592.

Zhong Q, Chen CF, Li S, Chen Y, Wang CC, Xiao J, Chen PL, Sharp ZD and Lee WH. (1999). *Science*, **285**.

Zhu Y, Qi C, Jain S, Le Beau MM, Espinosa III R, Atkins GB, Lazar MA, Yeldandi AV, Rao MS and Reddy JK. (1999). *Proc. Natl. Acad. Sci. USA*, **96**, 10848–10853.

In vivo potentiation of human oestrogen receptor α by Cdk7-mediated phosphorylation

Saya Ito[1], Ken-ichi Takeyama[1,2], Ayako Yamamoto[1], Shun Sawatsubashi[1], Yuko Shirode[1,2], Alexander Kouzmenko[1,2], Tetsuya Tabata[1] and Shigeaki Kato[1,2,*]

[1]*The Institute of Molecular and Cellular Biosciences, University of Tokyo, Bunkyo-ku, Tokyo, Japan*
[2]*SORST, Japan Science and Technology, Kawaguchi, Saitama, Japan*

Phosphorylation of the Ser[118] residue in the N-terminal A/B domain of the human oestrogen receptor α (hERα) by mitogen-activated protein kinase (MAPK), stimulated via growth factor signalling pathways, is known to potentiate ERα ligand-induced transactivation function. Besides MAPK, cyclin dependent kinase 7 (Cdk7) in the TFIIH complex has also been found to potentiate hERα transactivation *in vitro* through Ser[118] phosphorylation. To investigate an impact of Cdk7 on hERα transactivation *in vivo*, we assessed activity of hERα in a wild-type and *cdk7* inactive mutant *Drosophila* that ectopically expressed hERα in the eye disc. Ectopic expression of the wild-type or mutant receptors, together with a green fluorescent protein (GFP) reporter gene, allowed us to demonstrate that hERα expressed in the fly tissues was transcriptionally functional and adequately responded to hERα ligands in the patterns similar to those observed in mammalian cells. Replacement of Ser[118] with alanine in hERα (S118A mutant) significantly reduced the ligand-induced hERα transactivation function. Importantly, while in *cdk7* inactive mutant *Drosophila* the wild-type hERα exhibited reduced response to the ligand; levels of transactivation by the hERα S118A mutant were not affected in these inactive *cdk7* mutant flies. Furthermore, phosphorylation of hERα at Ser[118] has been observed *in vitro* by both human and *Drosophila* Cdk7. Our findings demonstrate that Cdk7 is involved in regulation of the ligand-induced transactivation function of hERα *in vivo* via Ser[118] phosphorylation.

Introduction

It is thought that most of the wide variety of oestrogen action is mediated through the transcriptional control of target genes by nuclear oestrogen receptor (ER) (Couse & Korach 1999; Ciana *et al.* 2003). The two subtypes of ER, α and β, belong to the nuclear receptor superfamily and act as ligand-induced transcription factors. As in other nuclear receptor superfamily members, structure of ER proteins is divided into five or six functional domains (designated as A to E/F domains). The highly conserved DNA binding domain is located in the C domain, while the ligand-binding domain (LBD) is mapped to the E/F domain. Transactivation function is present in the N-terminal A/B domain (AF-1) and in the C-terminal LBD (AF-2) (Kumar *et al.* 1987; Tora *et al.* 1989). Although both AF-1 and AF-2 are involved in the ligand-dependent transactivation function of ERs, AF-1 is constitutively active, while AF-2 activity is dependent on ligand binding (Endoh *et al.* 1999; Kobayashi *et al.* 2000; Watanabe *et al.* 2001). AF-1 and AF-2 domains have distinctive properties and their activities may depend on cell type and promoter context (Kumar *et al.* 1987; Tora *et al.* 1989).

ER target gene promoters contain oestrogen-response elements (EREs) that are recognized and directly bound by ER homo- or hetero-dimers followed by chromatin remodelling, presumably by recruited ATP-dependent chromatin remodelling complexes (Belandia & Parker 2003; Kitagawa *et al.* 2003). ERE-bound liganded ERs also induce recruitment of a number of histone acetyltransferase (HAT) and non-HAT cofactors that activate transcription (McKenna & O'Malley 2002). HAT coactivator complexes, CBP/p160 (Onate *et al.* 1995; Kamei *et al.* 1996; Chen *et al.* 1997; Spencer *et al.* 1997) and TRRAP/GCN5 (Yanagisawa *et al.* 2002), and non-HAT DRIP/TRAP complexes (Fondell *et al.* 1996;

Communicated by: Kohei Miyazono
**Correspondence*: Email: uskato@mail.ecc.u-tokyo.ac.jp

DOI: 10.1111/j.1365-2443.2004.00777.x

Yuan *et al.* 1998; Naar *et al.* 1999; Rachez *et al.* 1999) are thought to act as common coactivator complexes for ERs as well as for other DNA-binding transcription factors. Therefore, ligand binding leads to structural alteration and switch of ER function from transcriptional repression to transcriptional activation via the recruitment of coactivators (Shiau *et al.* 1998; Freedman 1999; Glass & Rosenfeld 2000; Metivier *et al.* 2003).

It is well known that phosphorylation of ERα modulates the activity of both AF-1 and AF-2 (Ali *et al.* 1993; Le *et al.* 1994; Kato *et al.* 1995; Chen *et al.* 2000). Among sites of potential phosphorylation, Ser^{118} residue (S118) in the hERα AF-1 domain has been particularly intensively studied with regard to the state of its phosphorylation and consequent potentiation of AF-1 activity. We have previously demonstrated that Ser^{118} is phosphorylated by ERK, a MAPK activated by the epidermal growth factor (EGF) or insulin-like growth factor (IGF) signalling, that results in the AF-1 potentiation in cultured cells (Kato *et al.* 1995). More recently, Chen and colleagues have shown that Cdk7 also phosphorylates hERα Ser^{118} in an oestrogen-dependent manner and enhances ERα transactivation in mammalian cells in culture (Chen *et al.* 2000). As Cdk7 is a key subunit of the basal transcription factor TFIIH complex (Frit *et al.* 1999; Egly 2001), it has been suggested that this phosphorylation takes place when TFIIH is recruited adjacent to hERα, presumably in the transcription initiation complex. Therefore, accumulating evidence suggests that phosphorylation of hERα Ser^{118} may play a significant role in regulation of AF-1 activity. However, the physiological role of Ser^{118} phosphorylation and associated kinases in hERα function remain to be established *in vivo*.

In *Drosophila melanogaster*, at least 20 members of the nuclear receptor (NR) family, such as the ecdysone receptor (EcR), have been genetically identified that, similar to the vertebrate NRs, are thought to transcriptionally control expression of target genes (Talbot *et al.* 1993; Baker *et al.* 2003). Recently, we reported that human androgen receptor ectopically expressed in *Drosophila* tissues was transcriptionally active and responsive to AR agonists and antagonists (Takeyama *et al.* 2002). In the present study, to assess an impact of Ser^{118} phosphorylation by Cdk7 and related kinases on hERα activity *in vivo*, we generated transgenic *Drosophila* lines in which hERα was ectopically expressed in specific *Drosophila* tissues using a GAL4/UAS system (Brand & Perrimon 1993). hERα expressed in the fly was transcriptionally functional and responded adequately to ER ligands, as expected from mammalian studies. Apparently, for its transactivation function in these transgenic flies, hERα recruited endogenous co-activators, such as those shown to be homologous to mammalian CBP and AIB1 (Akimaru *et al.* 1997; Bai *et al.* 2000). We found that replacement of S118 with alanine residue (S118A) in hERα resulted in the marked reduction of ligand-induced hERα transactivation in transgenic fly eye disc. Furthermore, in a *cdk7* inactive mutant *Drosophila* (*cdk7*^{a}) (Larochelle *et al.* 2001), transactivation by the wild-type but not the S118A hERα was significantly reduced. In addition, both human and *Drosophila* recombinant Cdk7 were equally able to phosphorylate hERα at Ser^{118} *in vitro*. We have also shown that Cdk7 acts as a co-activator of hERα transactivation in transfected cells in culture. Therefore, our results provide for the first time genetic evidence that phosphorylation of Ser^{118} potentiates transcriptional activity of hERα and that Cdk7 is involved in regulation of the ligand-induced transactivation function of hERα *in vivo* through Ser^{118} phosphorylation.

Results

hERα in *Drosophila* is transcriptionally functional

Our previous studies showed that human androgen receptor ectopically expressed in *Drosophila* tissues was adequately functional (Takeyama *et al.* 2002). We have utilized the same strategy to generate transgenic *Drosophila* expressing hERα together with ERE-dependent green fluorescent protein (GFP) as a reporter gene. Wild-type hERα (HEG0), AF-1 (HE15) or AF-2 (HE19) domains (as illustrated in Fig. 1A) were ectopically expressed in photoreceptor cells under control of the glass multimer reporter (*GMR*) gene promoter (Moses & Rubin 1991) using the *Drosophila melanogaster GAL4-UAS* system (Brand & Perrimon 1993). The eye disc, one of several larval discs in *Drosophila*, has been shown to be an effective model to assess Cdk7 function as a cell survival signal. Expression of hERα proteins was estimated by staining with immunofluorescent antibody. Levels of GFP reporter expression in respective eye discs were quantified by green fluorescence and normalized against the levels of ERα protein to determine fold of activation.

Dietary administration of 17β-oestradiol (E2) for 5 days from hatching remarkably induced GFP expression (Fig. 1B). The partial oestrogen agonist tamoxifen (TAM) and pure antagonist ICI182.780 exhibited partial oestrogenic and anti-oestrogenic actions, respectively, similar to that observed in mammals (McDonnell *et al.* 1995). E2-dependent (AF-2) and -independent (AF-1) transactivation functions were observed in the C-terminal-LBD and N-terminal A/B domain expressing transgenic flies, respectively, as expected from previous studies (Kumar *et al.* 1987; Tora *et al.* 1989; Kobayashi *et al.* 2000; Watanabe

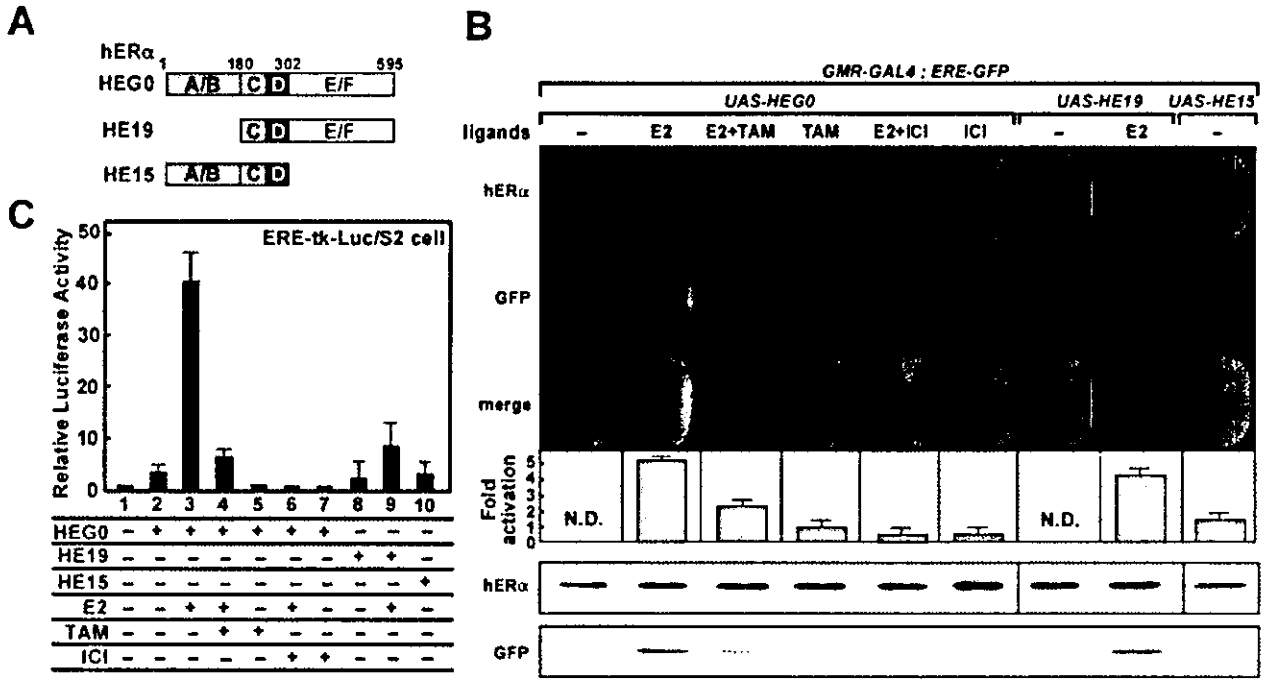

Figure 1 Ligand dependent transactivation of hERα in *Drosophila*. (A) Schematic representation of hERα constructs. The DNA binding domain (DBD) is located in the C domain (grey box). The transactivation function-1 (AF-1) region is located in the N-terminal A/B domain (blue box), while the transactivation function-2 (AF-2) region is located in the C-terminal E/F domain (white box) that also contains the ligand binding domain (LBD). (B) Ligand-dependent transactivation of hERα mutants in eye imaginal discs. Expression of hERα mutants in third instar larva eye discs driven by *GMR-GAL4* was detected with ERα antibodies (B10 or HC-20) (red). Transactivation of hERα mutants was estimated by GFP expression (green). The anterior is to the right. Bottom panels: hERα and GFP expression in four pairs of adult heads as detected by Western blotting. Fold-activation was calculated using hERα expression levels as normalizing factor. Ligands, 10^{-3} M 17β-oestradiol (E2), 10^{-2} M tamoxifen (TAM), and 10^{-2} M ICI 182.780 (ICI), were added in 100 μL of vehicle on top of 10 mL of the medium before hatching. Flies were kept at 25 °C. (C) Measurement of hERα mutants transactivation in Schneider cells. Schneider cells were transfected with hERα mutant expression plasmids, Actin-GAL4 plasmid, ERE-tk-luc reporter plasmid and pRL-CMV internal control plasmid in the presence or absence of 10^{-8} M E2, 10^{-8} M TAM or 10^{-8} M ICI. Firefly luciferase activity (ERE-tk-luc) was measured and normalized against Renilla activity (pRL-CMV-luc) as an internal control. Data are shown as the average and standard deviation of three independent experiments.

et al. 2001). Similar hER ligand effects and hERα AF-1 and AF-2 activities were observed in Schneider (S2) cells derived from *Drosophila* embryos (Fig. 1C). These data indicated that hERα ectopically expressed in *Drosophila* tissues was adequately functional in ligand-induced transactivation, presumably through recruitment of endogenous co-regulators. Therefore, it appears that human steroid receptors ectopically expressed in *Drosophila* retain their transactivation function.

Co-activation of hERα by *Drosophila* CBP and p160 HAT homologues

As hERα was transcriptionally functional in insect cells in culture and in *Drosophila* eye disc cells *in vivo*, ability of endogenous fly co-activators to modulate hERα transactivation was assessed in mutant flies deficient for *Drosophila* homologues of mammalian p160 (*tai*) or CBP (*nej*) (Akimaru *et al.* 1997; Bai *et al.* 2000). The oestrogen-induced transactivation function of hERα was clearly reduced in both of these mutants without affecting levels of hERα expression (Fig. 2). These data suggest that *Drosophila* homologue of the mammalian p160/CBP HAT complex acts as a co-activator of hERα in the fly cells. This was further confirmed by the observation of enhanced hERα transactivation in flies over-expressing TAI, *Drosophila* AIB1 homologue, in the eye disc.

The p160/CBP HAT complex has been shown to activate hERα AF-2 via the direct association of p160 family member proteins with helix 12 of the hERα LBD (Onate *et al.* 1995; Chen *et al.* 1997; Heery *et al.* 1997). However, little is known about the role of the

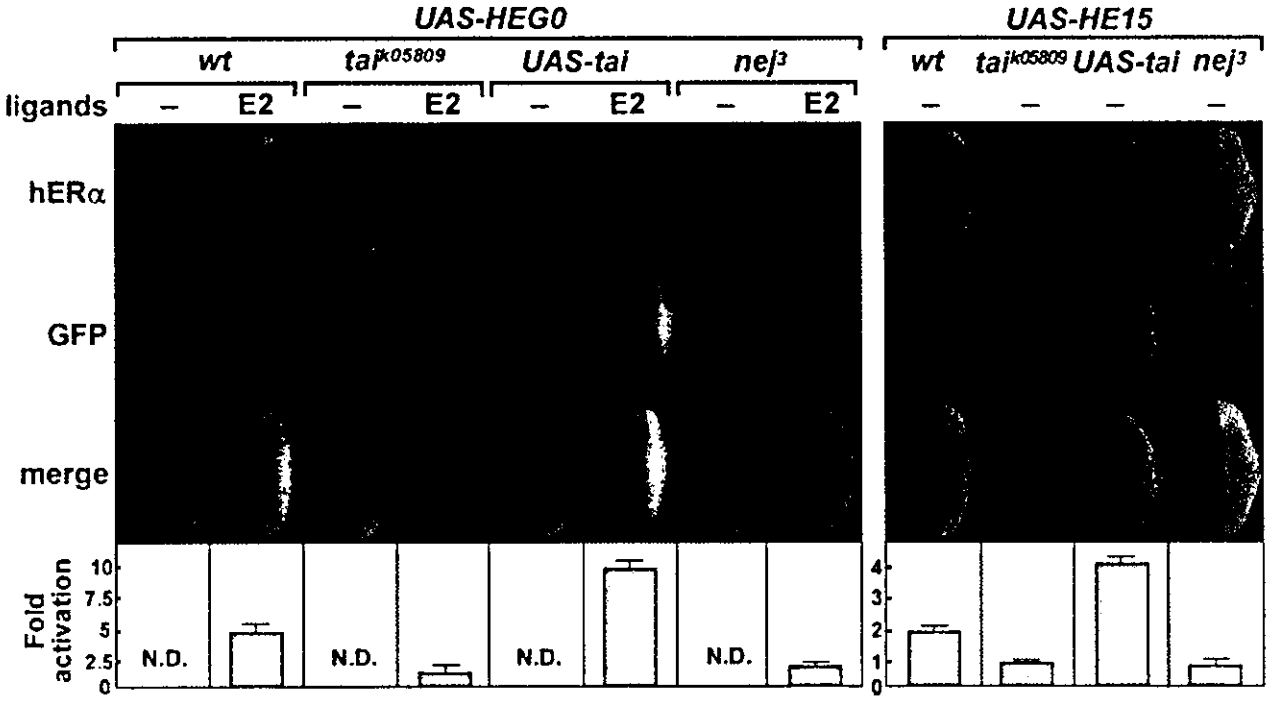

Figure 2 hERα transactivation regulated by *Drosophila* transcriptional co-activators. hERα expression (red) and transactivation (green) were visualized by immunostaining with ERα antibodies (B10 and HC-20) and GFP expression, respectively, in eye imaginal discs. Fly lines contained single copies of *GMR-GAL4*, *UAS-hERα* (*HEG0* or *HE15*) and *ERE-GFP* with or without heterozygous tai^{k05809}, *UAS-tai* or nej^{3}.

p160/CBP complex in modulation of hERα AF-1 activity. Although it is presumed that the complex bridges the AF-1 and AF-2 domains to synergistically enhance hERα transactivation function (Kobayashi *et al.* 2000), the p160/CBP complex was also able to enhance transcriptional activity of the AF-1 domain alone (i.e. the HE15 mutant). Indeed, similar patterns of AF-1 domain (HE15) and full-length hERα (HEG0) transactivation in mutant flies (Fig. 2) suggest that hERα AF-1 activity is modulated *in vivo* by the p160/CBP co-activator complex.

Significant role of Ser^{118} in hERα function *in vivo*

In mammalian cells, the potentiation of hERα AF-1 by phosphorylation of the Ser^{118} residue has been well documented (Kato *et al.* 1995; Chen *et al.* 2000). However, the impact of Ser^{118} phosphorylation in hERα transactivation function has not yet been verified *in vivo*. We tested the significance of hERα Ser^{118} in the insect S2 cells transfected with hERα mutants containing a serine to alanine replacement at position 118 (HE457, HE15/457) (Fig. 3A and 3B). These mutants exhibited decreased transactivation capacities even though levels of the mutant expression appeared to be similar to that of wild-type hERα.

We then examined the role of Ser^{118} in hERα function in transgenic flies (Fig. 3C). Although mutant and wild-type hERα expression levels in third instar larval eye discs were indistinguishable, a clear reduction in GFP induction was observed in the alanine replacement mutants. These findings provided evidence that the Ser^{118} residue played a pivotal role in hERα transactivation *in vivo*.

In vivo potentiation of hERα by Cdk7-mediated phosphorylation at Ser^{118}

As it is likely that the Ser^{118} residue could be phosphorylated by a number of endogenous protein kinases to support hERα transactivation, we studied the ability of dCdk7 to phosphorylate hERα at Ser^{118} *in vitro* and *in vivo*. The serine/threonine kinase Cdk7 is indispensable for transcription initiation by RNA polymerase II as an essential component of the transcription factor TFIIH complex (Frit *et al.* 1999; Egly 2001). $dcdk7^{ts}$ mutant flies express a temperature-sensitive Cdk7 mutant that is inactive at temperatures at or above 30 °C (Larochelle *et al.* 2001). We assessed transactivation function of HEG0 and HE457 in these $dcdk7^{ts}$ mutant flies (Fig. 4, left panel). Oestrogen-induced transactivation of